HIGH RESOLUTION SPECTROSCOPY OF SHORT PERIOD PULSATING STARS

BALAGE DHANAL NIRMALA PERERA

A dissertation submitted in partial fulfilment of the requirements for the Bachelor of Science
Special Degree in Physics

of the

University of Colombo, Sri Lanka

JANUARY 2018

DECLARATION

I certify that this dissertation does not incorporate without acknowledgement, any material previously submitted for a Degree or Diploma in any university and to the best of my knowledge and belief it does not contain any material previously published or written or oral communicated by other person except where due reference is made in the text.

....

B.D.N. Perera

ACKNOWLEDGEMENT

ABSTRACT

Spectrometric and photometric studies are used comprehensively by researchers throughout the world to gather information. However due to the limited facilities in Sri Lanka, researches in this field is still developing. A spectroscopic data analysis was done throughout this project on HD67930 δ Scuti variable Star, as less number of spectroscopic experiments were carried out in the past.

Spectroscopic images of rapidly rotating δ Scuti star HD67930 were taken during 17 Oct, 2016 and 18 Oct, 2016 using the 50cm Corrected Dall-Kirkham reflector telescope at Mount Abu Infrared observatory, India were analyzed using IRAF software.

Variable stars emit spectra with absorption lines due to presence of corresponding elements in their atmosphere. The research is very subtle since amazing facts about these distance variable stars can be obtained using the spectral lines.

The determined corresponding wavelengths of absorption lines were H(α) = (6560 $\pm$ 1) ^{0}A, H(β)= (4862 $\pm$ 1) ^{0}A, H(γ) = (4351 $\pm$ 1) ^{0}A and Fe^{3+} = (6869 $\pm$ 1) ^{0}A. Which provides the fact that these elements exist in the star atmosphere.

The graphs of Equivalent width vs phase and Full width at half maximum vs phase were plotted to each and every absorption line in order to model their variation with phase,mathematically.

TABLE OF CONTENT

LIST OF FIGURES

LIST OF TABLES

ABBREVIATIONS

CCD   − Charged Coupled Device

IRAF   − Image Reduction and Analysis Facility

DCST   − Delta Scuti Stars

FWHM   − Full Width at Half Maximum

JD   − Julian Date

HJD   − Heliocentric Julian Date

H-R   − Hertzaprung Russel Diagram

NOAO   − National Optical Astronomy Observatory

FITS   − Flexible Image Transportation System

UTC   − Universal Time Cordinates

ADU   −Analog to Digital Units

1 INTRODUCTION

In early days people were inquisitive to know about the sky, stars and planets above us. Therefore they started searching for celestial objects. Which laid the foundation to the astronomy. Astronomy is not only the oldest of all sciences, also it can be called the fountainhead of all sciences. The solution for the planetary motion give rise to mechanics, the first systematized branch of physics. The interaction stellar structures, thermonuclear processes and testing of general theory of relativity by astronomical observation of the remote galaxies and quasars are some of the branches of science where astronomy and physics goes together in order to get familiar with the universe which we lives.

As events occur automatically in space, astronomy is a more observational science with comparing to the experimental sciences which we control the conditions of the experiment. Without doubt our telescopes are capable of probe in to deep space. But question lies within "Are they capable of investigating the interior of the sun and stars?" In early astronomy it was believed that interior of stars are less accessible to scientific investigation. More like it is almost impossible to determine interior of the stars.

In modern astronomy scientists have discovered a method to discover stellar interior using acoustic oscillations and seismic waves. Which gave rise to a quite different field from astronomy called "Asteroseismology".

1.1 Stars

A star is made out of positively and negatively charged particles which are in the state of matter called plasma. This plasma is held together by massive amount of gravity. A star shines due to fusion of hydrogen into helium inside the core and energy is transferred from core to the outer layers.

1.1.1 Variable and pulsating stars

Nearly all the physical processes that determine the structure and evolution of stars occur in their (deep) interiors. The production of nuclear energy that powers stars takes place in their cores for most of their lifetime. The effects of the physical processes that modify the simplest models of stellar evolution, such as mixing and diffusion, also predominantly take place in the inside of stars.

The light that we receive from the stars is the main information that astronomers can use to study the universe. However, the light of the stars is radiated away from their surfaces, carrying no memory of its origin in the deep interior. Therefore it would seem that there is no way that the analysis of starlight tells us about the physics going on in the unobservable stellar interiors.

However, there are stars that reveal more about themselves than others. Variable stars are objects for which one can observe time-dependent light output, on a time scale shorter than that of evolutionary changes. There are two major groups of variable star, extrinsic and intrinsic variables.

Extrinsic variables do not change their light output by themselves. For example, the light changes of eclipsing binary stars are caused by two stars passing in front of each other, so that light coming from one of them is periodically blocked. The individual components of eclipsing binary stars are not necessarily variable. By analyzing the temporal light variations and orbital motion of eclipsing binaries, one can determine their fundamental properties, and by assuming that their components are otherwise normal stars, determine fundamental properties of all stars, most importantly their masses. In this way, stars and stellar systems can be understood better.

Intrinsic variables, on the other hand, change their light output physically. Supernovae, which are stellar implosions/explosions, can become brighter than their host galaxies because of the ejection of large amounts of material. Even more revealing are stars that vary their sizes and shapes.

With the ever increasing precision in photometric and radial velocity measurements, a large number of groups of pulsating star is nowadays known. Figure 1 shows theoretical (in the sense that the logarithm of the effective temperature is plotted versus the logarithm of the stellar luminosity) HR Diagrams containing the regions in which pulsating stars were known some 40 years ago and today.
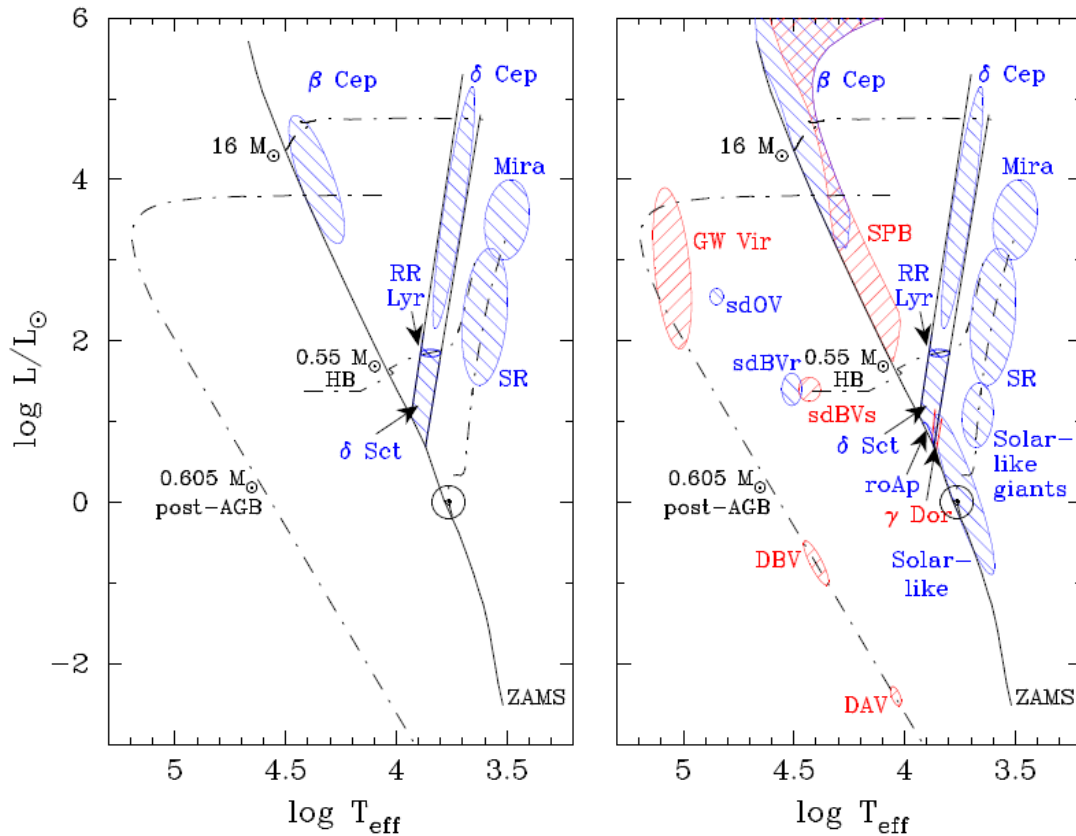
Figure 1.1 Theoretical HR diagram schematically showing locations of selected confirmed

The different types of pulsating stars have historically been classified on a phenomenological basis. The separation between those types has usually later turned out to have a physical reason. The individual classes are different in terms of types of excited pulsation mode (or, less physical, pulsation period), mass and evolutionary state, hence temperature and luminosity. The names of these classes are assigned either after the name of a prototypical star or give some description of the type of variability and star.

It must be pointed out that the present overview does not contain all types and subgroups of pulsating star that have been suggested.

1. Cepheids
2. RR Lyrae
3. RV Tauri
4. LPVs

3

The Cepheids are subdivided according to population and evolutionary state into,

1. δ Cephei
2. W Vir
3. RV Tau
4. BL Her

The classification of and distinction between the different classes of pulsating star, that are historically grown and modified designations, can in some cases be called arbitrary today, one recognizes an important fact that pulsating stars populate almost the entire HR diagram, and this means that they can be used to learn something about the physics of most stars.

1.2   Spectral Classification

In the study of stars, it is of great convenience to have some sort of classification system. Modern classification of stars is based on its spectral characteristics. Light from the star is analyzed by splitting it up from a diffraction grating thus dividing the incoming light in to its constituent wavelengths. Generally the spectrum consistent of absorption lines superimposed on the continuum. Each line indicates the presence of a certain ion of a certain chemical element. The presence of certain chemical element in such an absorption spectrum indicates that the temperature conditions are suitable for a certain excitation of this elements.

The current accepted classification system is mainly based on temperature where stars are classified using the letters O, B, A, F, G, K and M. The hottest being O and M being the coolest. The letter sequence indicates successively the decrease in temperature O to M.

Table 1.1 Spectral Classification

Spectral Class	Surface Temperature
O	28,000-50,000
B	10,000-28,000
A	7,500-10,000
F	6,000-7,500
G	4,900-6,000
K	3,500-4,900
M	2,000-3,500

1.3   Types of astronomical spectra

Spectroscopy is probably the most important tool used in the field of astronomy. Almost all the properties of stars that the scientists talk of are determined by analyzing their spectra. Basically three types of spectrums have been found to exist. They are,

1. Continuous spectrum
2. Absorption spectrum
3. Emission spectrum

1.3.1   Continuous Spectrum

A dense hot object such as the core of a star acts like a black body radiator. If light from the source is viewed directly without any intervening matter then the resultant spectrum would appear to be a continuum.

1.3.2   Absorption Spectrum

Most stars are surrounded by outer layers of gays that are less dense than the core. The photon emitted from the core cover all frequencies. Photon of specific frequency can be absorbed by electrons in the diffuse outer layer of gas, causing the electron to charge energy levels. Eventually the electron will de-excite and jump down to a lower energy level, emitting a new photon of a specific frequency. The direction of the re-emission however is random so the chance of it traveling in the same path as the original incident photon are very small. The net effect is to reduce the intensity of light at the wavelength of that photon in the direction of the

observer. This leads the resultant spectrum to show dark absorption lines showing a decrease in intensity. Most stellar spectra typically are of this kind.

1.3.3 Emission Spectra

Emission spectrums occur if an observer is not looking directly at the source but instead at a diffuse cloud of gas. If this cloud is excited by a nearby energy sources such as hot, young stars, then the electron in atoms of the gas cloud can get excited. When they de-excite they emit photon of specific frequency. As these photons can re emit in any direction, an external observer will detect light at these wavelengths. The spectrum formed this way is an emission or spectrum.

1.4 SZ Lyncis (HD67930)

SZ Lyncis (RA=08h 09m 35.8s, DEC=$+44^0$ 28' 17.6") is a high amplitude δ Scuti type binary star which has pulsation period of 0.1205 days and orbital period of 1173.5 days (Soliman et al., 1986). The pulsating star is the brighter component while the faint component could not be observed in spectroscopy and characterized as single line spectroscopic binary (Gazeas et al., 2004). The star has been analyzed for the periodic variations in number of times and found that the pulsation period changes $2.25\pm0.42\times10^{-12}$ days per cycle (Paparo et al., 1988). Most of the observation considered the main pulsation period and a few attempts have been made to investigate the harmonics and secondary periods.

2 BACKGROUND

2.1 Discovery of Pulsating Stars

The first pulsating star was discovered more than 400 years ago. In 1596 David Fabricius remarked that the star o Ceti (subsequently named "Mira", the wonderful) disappeared from the visible sky. About 40 years later, it was realized that it did so every $\sim$ 11 months; the first periodic variable star was known (although we know today that in this case, the term "periodic" is not correct in a strict sense).

In 1784 John Goodricke discovered the variability of δ Cephei, and in 1914 enough evidence had been collected that Harlow Shapley was able to demonstrate that the variations of δ Cephei and related stars (also simply called "Cepheids") was due to radial pulsation. Also in the teens of the previous century, Henrietta Leavitt pointed out that the Cepheids in the Small Magellanic Clouds follow a period-luminosity relation, still one of the fundamental methods to determine distances in the visible universe - and one of the major astrophysical applications of pulsating stars.

Table 2.1 gives a rough overview of the classes of pulsating stars.

Table 2.1 Classes of Pulsating Stars

Name	Approximate Periods	Discovery
Mira variables	100 - 1000 d	Fabricius (1596)
Semiregular (SR) variables	20 - 2000 d	Herschel (1782)
δ Cephei stars	1 - 100 d	1784, Pigott, Goodricke (1786)
RR Lyrae stars	0.3 - 3 d	Fleming (1899)
δ Scuti stars	0.3 - 6 h	Campbell & Wright (1900)
β Cephei stars	2 - 7 h	Frost (1902)
ZZ Ceti stars (DAV)	2 - 20 min	1964, Landolt (1968)
GW Virginis stars (DOV)	5 - 25 min	McGraw et al. (1979)
Rapidly oscillating Ap (roAp) stars	5 - 25 min	1978, Kurtz (1982)
V777 Herculis stars (DBV)	5 - 20 min	Winget et al. (1982)
Slowly Pulsating B (SPB) stars	0.5 - 3 d	Waelkens & Rufener (1985)
Solar-like oscillators	3 - 15 min	Kjeldsen et al. (1995)
V361 Hydrae stars (sdBVr)	2 - 10 min	1994, Kilkenny et al. (1997)
γ Doradus stars	0.3 - 1.5 d	1995, Kaye et al. (1999)
Solar-like giant oscillators	1 - 18 hr	Frandsen et al. (2002)
V1093 Herculis stars (sdBVs)	1 - 2 hr	Green et al. (2003)
Pulsating subdwarf O star (sdOV)	1 - 2 min	Woudt et al. (2006)

2.2   Astronomical Spectroscopy

Many of the atoms from which our bodies are made were once, thousands of millions of years ago, deep in the interior of one of many stars which have long since either blown themselves into pieces, or perhaps faded quietly into obscurity. The most interesting question to be asked is how astronomers and physicists have uncovered this fascinating story by looking at the sky and working in the laboratory. Much of it has been pieced together using the techniques of astronomical spectroscopy.

2.2.1   Spectra and their Importance to the Astrophysics

It is interesting to know that, how scientists gather so much of knowledge about the chemical compositions, temperatures, pressures and motions of nebulae, galaxies and other stellar objects which are very so distant that we would never dream of trying to travel to them. In order to answer this question we have first to ask how we know that these bodies exist at all. Quite simply, we know that they exist because we can see them; i.e. they are emitting energy in the form of light waves and also infrared, ultraviolet and often radio waves and X rays as well. This energy provide us an extremely rich source of information about their makeup. A spectrum is the result of splitting up this light into its constituent colors and it is by studying spectra that astrophysicists have been able to make their most important discoveries.

2.2.2   Formation of Spectrum

The most familiar spectrum in nature is the rainbow, which is produced when light from the sun bounces around inside each of millions of raindrops and gets sorted out into its constituent colors in the process. When the chemist, physicist or astronomer wishes to examine a source of light he may use a triangular glass prism, or more commonly nowadays a device called a spectrum. The whole apparatus for doing this job is called a spectroscope, or a spectrograph (if the spectrum is recorded photographically or by some means other than the eye). All modern spectrographs use diffraction gratings which can give excellent results.

2.2.3 Information that can be extracted from a Spectrum

In the early days of 16th century astrophysicists realized that the colors produced when white light is passed through a prism are the property of the light itself, rather than something introduced by the glass. This realization was to have extremely far reaching consequences for the whole of physics and for our understanding of the universe in particular.

The great revolution in physics which took place during the first few decades of this century led to a thorough understanding of the way in which atoms and molecules can absorb and emit light and other radiations. It was known long before those different chemical elements emitted their own characteristic colored radiations or lines when heated In their gaseous state, but it was the understanding of the relationship between those lines and the structure of the atoms or molecule that provide to be so important for the development of astrophysics.

If we look at an astronomical spectrum, and see the lines characteristic of a particular elements, then we can immediately say that elements is present either in the nebula itself or, in the space between the nebula and our telescope. This is important and exiting enough itself but, so powerful are the techniques of spectroscopy that we can do much more than just detect the presence of a chemical element or molecule. Obviously next to found out is the quantity of each element present in a particular nebula. In fact this is not a very easy question to be answered, but it can be done using a sophisticated methodology.

The spectrographs makes a major contribution to the study of the motions of astronomical objects too. If we want to see how fast a galaxy moves away from us, we can simply use the Doppler principal. All we have to do is to measure the stellar lines from the corresponding lines produced in a lamp mounted in the spectrograph. This procedure has the very important advantage that we do not have to know the distance to the galaxy at all which is very difficult to measure. This means that we can measure the velocities of galaxies and nebulae that are so very far away that any proper motion would be immeasurably small.

The radial velocities have been measured for many thousands of stellar objects in our galaxy and this is leading to an understanding of its formation and evolution. For instance we know that the sun makes an almost circular orbit around the center of the galaxy once every 250 million years but at the same time some very much older stars move in different, non-circular orbits as well.

2.3   Julian Date (JD)

Julian dates are simply a continuous count of days and fractions since noon Universal Time on **January 1, 4713** BC (on the Julian calendar). Almost 2.5 million days have transpired since this date. Julian dates are widely used as time variables within astronomical software.

2.3.1   Heliocentric Julian Date (HDJ)

The Heliocentric Julian Date is the Julian Date adjusted to the center of the Sun. It depends on the JD of the observation and the celestial coordinates of the object.

3   THEORY

In spite of the enormous size, the stars can oscillate. For the oscillations of the stars, there is fundamental mode of oscillation as well as the harmonics. The fundamental mode is the expansion and contraction of the star in radial direction. The figure 2.1 (a) shows the fundamental mode of oscillation analogy with radial oscillation and figure 2.1 (b) shows the oscillations analogy with non-radial oscillations.
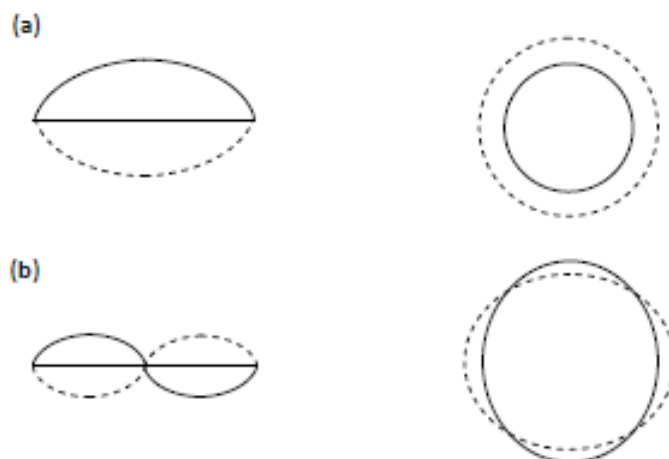
Figure 3.1 Radial and non-radial oscillation of a star

3.1   Pressure Modes and Gravity Modes

There is more to stellar pulsation than acoustic waves – sound waves– in stars. Those acoustic waves are known as "pressure" modes, or p modes. There are equally important "gravity" modes, or g modes, where the restoring force of the pulsation is not pressure. Most of the stellar pulsations occur due to the gravity modes. But gravity modes are not acoustic. They are not caused by the sound waves in stars.

3.1.1   3-D Oscillations in Stars

Stars are three-dimensional, so their natural oscillation modes have nodes in three orthogonal directions. These are described by the distance r to the center co-latitude θ and longitude φ; here θ is measured from the pulsation pole, the axis of symmetry (hence is co-latitude, since latitude is measured from the equator). The nodes are concentric shells at constant r, cones of constant θ and planes of constant φ. For a spherically symmetric star the solutions to the equations of motion have displacements in the (r, θ, φ) directions and are given by,

$$\xi_r(r,\theta,\Phi,t) = a(r)Y_l^m(\theta,\Phi)e^{-2i\pi vt} \qquad (1)$$

$$\xi_r(r,\theta,\Phi,t) = b(r)\frac{\partial Y_l^m(\theta,\Phi)}{\partial \theta}e^{-2i\pi vt} \qquad (2)$$

$$\xi_r(r,\theta,\Phi,t) = \frac{b(r)}{\sin\theta}\frac{\partial Y_l^m(\theta,\Phi)}{\partial \Phi}e^{-2i\pi vt} \qquad (3)$$

Where ξr, $\xi\theta$ and $\xi\Phi$ are the displacements, $a(r)$ and $b(r)$ are amplitudes, v is the oscillation frequency and $Y_l^m(\theta,\Phi)$ are spherical harmonics given by,

$$Y_l^m(\theta,\Phi) = (-1)^m \sqrt{\frac{2l+1}{4\pi}\frac{(l-m)!}{(l+m)!}}P_l^m(\cos\theta)e^{im\Phi} \qquad (4)$$

Where $P_l^m(\cos\theta)$ Legendre polynomials. Given by,

$$P_l^m(\cos\theta) = \frac{1}{2^l l!}(1-\cos^2\theta)^{\frac{m}{2}}\frac{d^{l+m}(\cos^2\theta-1)^l}{d\cos^{l+m}\theta} \qquad (5)$$

Spherical harmonics are defined such that integral of $|Y_l^m|^2$ over the unit sphere equal 1, as secured by the normalization constant,

$$C_{lm} = \sqrt{\frac{2l+1}{4\pi}\frac{(l-m)!}{(l+m)!}} \qquad (6)$$

3.1.2   Radial Modes

The simplest modes are the radial modes with $l = 0$, and the simplest of those is the fundamental radial mode. In this mode the star swells and contracts, heats and cools, spherically symmetrically with the core as a node and the surface as a displacement antinode. This is the usual mode of pulsation for Cepheid variables and for RR Lyrae stars, amongst others.

The first overtone radial mode has one radial node that is a concentric shell within the star. As we are thinking in terms of the radial displacement, that shell is a node that does not move, the motions above and below the node move in antiphase. As an example, in the roAp stars (which are nonradial pulsators) radial nodes can be directly observed in their atmospheres with just this kind of motion in antiphase above and below the radial node (Kurtz et al. 2005b). The surface of the star is again an antinode. There are Cepheid variables, RR Lyrae stars and δ Sct stars that pulsate simultaneously in the fundamental and first overtone radial modes. In the cases of the Cepheids and RR Lyrae stars they are known as double-mode Cepheids and RRd stars, respectively. For the Cepheids the ratio of the first overtone period to the fundamental period is 0.71, for the δ Sct stars it is 0.77.

This difference is profound and it is our first use of asteroseismology. If the star were of uniform temperature and chemical composition (so that the sound speed were constant).The larger ratios in the Cepheids and δ Sct stars are a direct consequence of the sound speed gradient in them, hence of the temperature and (in some places) of chemical composition gradients. The small, but significant differences between the Cepheid and δ Sct ratios are a consequence of the Cepheid giant star being more centrally condensed than the hydrogen core-burning δ Sct star. Thus, just by observing two pulsation frequencies we have had our first look into the interiors of some stars.

3.1.3   Nonradial Modes

The simplest of the nonradial modes is the axisymmetric dipole mode with $l = 1$, $m = 0$. For this mode the equator is a node; the northern hemisphere swells up while the southern hemisphere contracts, then vice versa; one hemisphere heats while the other cools, and vice versa – all with the simple cosine dependence of $P^0_1 (\cos \theta) = \cos \theta$, where θ is the co-latitude. There is no change to the circular cross-section of the star, so from the observer's point of view, the star seems to oscillate up and down in space.

Nonradial modes only occur for $n \geq 1$, so in the case of the $l = 1$ dipole mode, there is at least one radial node within the star. While the outer shell is displaced upwards from the point of view of the observer, the inner shell is displaced downwards and the centre of mass stays fixed. Dipole modes are the dominant modes observed in the rapidly oscillating Ap stars, and are also seen in many other kinds of pulsating variables.

Modes with two surface nodes ($l = 2$) are known as quadrupole modes. For the $l = 2$, $m = 0$ mode the nodes lie at latitudes $\pm 35^0$, since $P_0{}^2 (\cos\theta) = (3\cos^2\theta - 1)/2$. The poles of an $l = 2$, $m = 0$ mode swell up (and heat up, although not usually in phase with the swelling) while the equator contracts (and cools), and vice versa. Figure 3.1 represents and explains a set of octupole modes with $l = 3$, giving a mental picture of what the modes look like on the stellar surface which is generally inclined with respect to the line-of-sight.
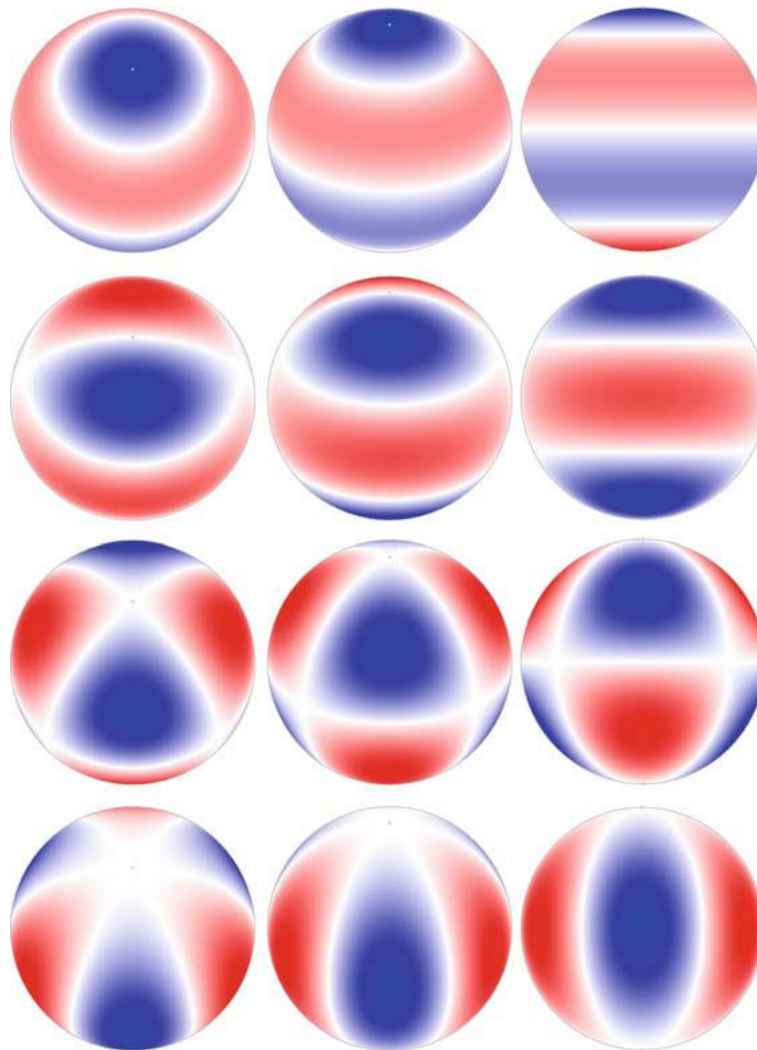
Figure 3.2 Illustration of modes in a star

4   INSTRUMENTATION

The observations were carried out at Mount Abu Infrared observatory. The observatory is located near the town of Mount Abu in the state of Rajasthan, India. The observatory is at 24.59° N, 72.71° E and an altitude of 1680 meters with typical astronomical seeing of ~ 1.2 arc seconds and is adjacent to Guru Shikhar, the highest peak of the Aravalli Range.

4.1   The 50cm CDK Reflector and CCD camera with filter Wheels

The Corrected Dall-Kirkham (CDK) has a 50 cm Prolate Ellipsoid, f/3 primary mirror and 19 cm spherical secondary mirror with the effective focal ratio of f/6.8 equatorial mount telescope. The detector is 1024 x 1024 electrons multiplying (EM) CCD with the maximum cooling of -80 C and negligible read noise. The higher frame rate per second and negligible read out noise (< 1 electron with EM gain) are ideal for the observation of short period variable stars with very high time resolution. The large CCD array provides a field of view 13 X 13 arc minutes which is an advantage to observe the entire cluster in single frame. In addition to the standard UBVRI filters, a set of Polaroid sheets oriented at 0, 45 and 90 degrees are also included in the system. The telescope and the dome are fully automated through the network and can be operated remotely from PRL with all functionalities including weather monitoring.

Figure 4.1 Mount ABU Observatory and 50cm CDK Reflector

4.2 LISA High Luminosity Slit based Spectrograph

A spectrograph is used to obtain and record astronomical spectrum. The difference between a spectrograph and a spectrometer is spectrograph has a mechanism to record the spectrum while a spectrometer allow us to observe the spectrum. A spectrograph is usually fitted in to the place where eye piece is located in the telescope. Most of the spectrographs are based on the same principle a light source (slit, see below) is collimated by a collimator lens, then spread out by an optical element (prism or grating), and refocused with an objective lens on a sensor (Camera CCD chip for instance) to form the spectrum.
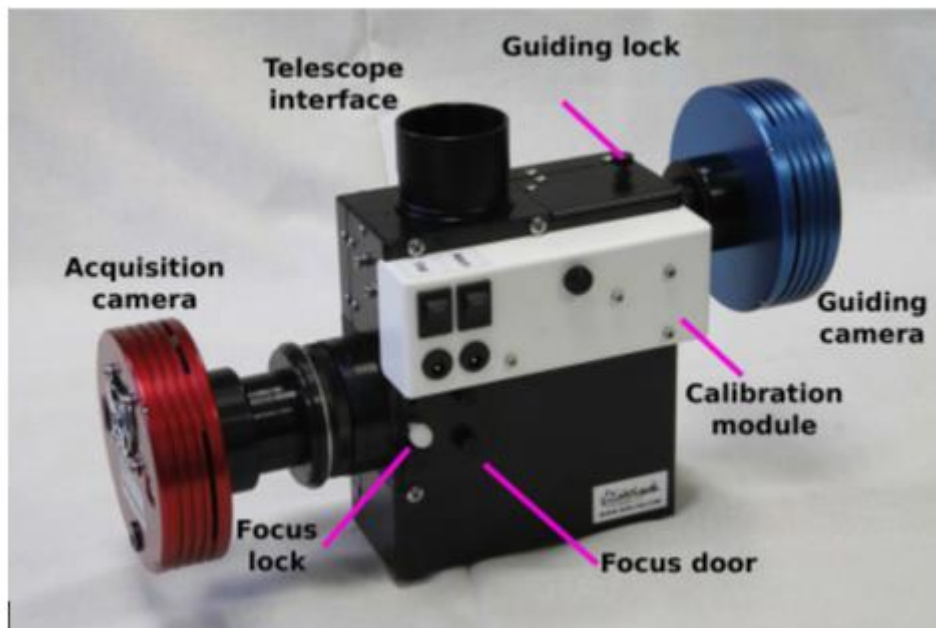
Figure 4.2 LISA Spectrograph
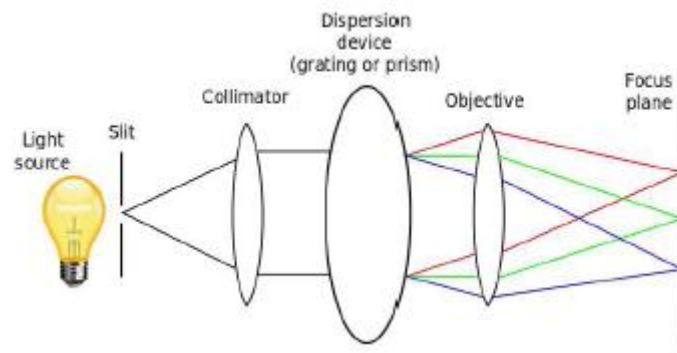
Figure 4.3 Mechanism of the Spectrograph

Spectroscopy is used in many applications. But spectroscopy applied to astronomy have some specificities,

1. The light source is usually faint: you must have an efficient optical system to take opportunity of each photon.
2. To get light from the source, you must use a telescope, which is moving at earth's speed.

Table 4.1 Specifications of LISA spectrograph

Range of wavelength	4000-7000 ^{0}A
Dispersion	5 ^{0}A/pixel
Collimator	Focal length of 130nm
Slit	Length: 4mm Width: 0-8mm
Dispersion system	Grating: Reflection type plane diffraction grating
Comparative light source	Ar-Ne light

4.3   CCD Camera

The introduction of CCD has dramatically changed the observation methods in astronomy. The highly sensitive detectors amplify the tiny current generated by photons heading from faint objects. The light sensing ability of CCD is 2.5mm a side. But it contains 32,680 light sensitive photo sites. Each photo site consists of silicon substrata overlaid with an insulating layer of silicon dioxide and a strip of   polysilicon above it. Within each sites the photo sites are separated by channel stops, a thin strip of silicon that has boron atoms implanted. The channel stops block the movement of electrons across columns within the silicon.

When light photons fall on the CCD, photons pass through the polysilicon and silicon dioxide layer in to the silicon. There they interacts with the atoms in the silicon crystal lattice, knocking electrons off the atoms according to the photo electric effect. The number of electrons knocked is proportional to number of photons collide on CCD. The average efficiency of a CCD is nearly 60%. The knocked electrons are trapped in potential well, which are regions in silicon

17

layer where the electric potential is at its maximum. In electronic terminology, the swarm of electrons become a charge packet trapped in a potential well.

4.3.1 Quantum Efficiency of the CCD

The quantum efficiency is defined as the ratio of the number of photons detected by the camera to the number of photons incident. It is obvious that the CCD doesn't work with the same efficiency in every wavelength.

4.4 IRAF Software

IRAF is an image processing software which is being widely used by professional astronomers and physicists around the world. IRAF provides a wide range of image processing tools for the user. And it is product of NOAO in USA.

The IRAF system has been designed basically to operate on UNIX based systems. The IRAF core system provides the user with a wide selection of image processing tools. Commands, call tasks can be executed to perform various functions. Each task has a parameter file that user can modify to affect the output of the task.

IRAF is designed to run on a terminal called "xgterm" and all executions are initiated through this terminal. IRAF also provides an interactive tool called "SAOImageDS9" which allows user to modify and perform various tasks related to images.

Main tasks performed by IRAF are,

1. Noise reduction of the images taken by CCD.
2. Calibration of stellar spectra
3. Photometric studies

IRAF has been designed to work with FITS image format.

4.5 Bias Frame

A bias frame is an image obtained with almost zero exposure time when the shutter of the CCD is closed. The image only contains noise due to the electronics that is inherent to the CCD chip.

4.6 Flat Fielding

Modern CCDs are uniform to neighboring photosites more than 1%. Even this value has significant effect in astronomy. If every photosite receives same amount of light, equal output current is expected from each and every photosite. Instead pixels show some variation. Therefore a frame called flat field has to be produced by taking the image of a uniformly illuminated surface such as white wall or a twilight sky. This flat field frames serves as a map of the CCD sensitivity and each photosite is corrected for sensitivity on each corresponding pixel.

By combining these effects, a raw image taken by the CCD consisting of above factors can be represented by the following equation.

$$Correted\ Image = \frac{Raw\ Image - Bias}{Flat\ Field} \tag{7}$$

5 METHODOLOGY

5.1 Data Reduction Analysis procedure

The analysis process for one spectrum is presented in this chapter. The following steps were involved in reducing data. A spectrum image of the HD67930 which belongs to SZ Lyncis constellation, obtained from the 50cm CDK reflector can be seen as follows.
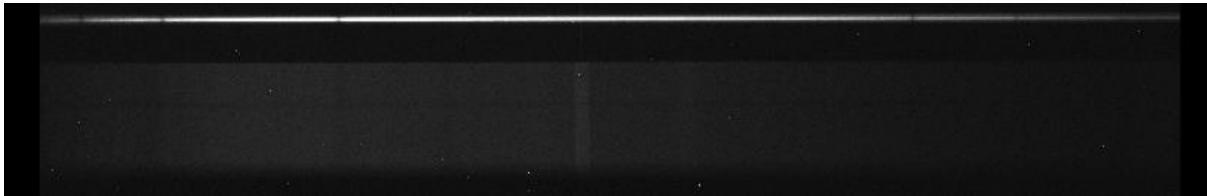
Figure 5.1 The CCD image of HD67930

Then the basic image reduction such as subtraction of bias frame and flat field correction was done to the spectrum image.
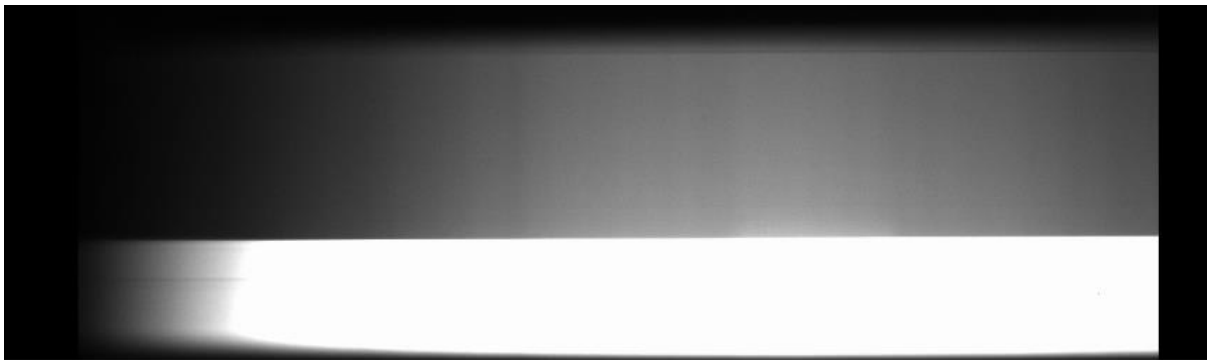
Figure 5.2 Flat Field Spectrum generated by spectrograph
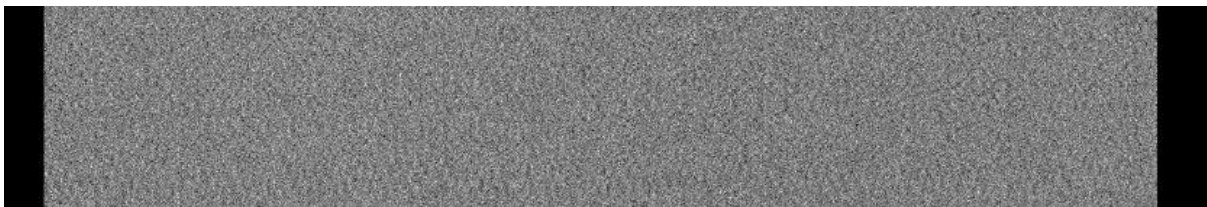
Figure 5.3 Bias frame spectrum generated by spectrograph

5.1.1 Extraction of a 1-D spectrum

The raw spectrum is a 2D image. It is convenient to have a 1D spectrum for the analysis. Therefore a 1D spectrum was obtained using the task called "appal" in IRAF. When the appal task is executed, the 2D spectrum is scanned in the x direction while summing few rows on either side of the centre of the spectrum to obtain a higher signal. In a 1D spectrum the intensity is available in ADU for each pixel in the x direction.

When using the appal task the extraction parameters must be changed according to the star. At the 1st stage of extraction the exact spatial centre of the stellar profile at some points along the dispersion axis was found. There are special parameters as saturation, readnoise and gain in appal task. Those parameters were adjusted according to the CCD image.
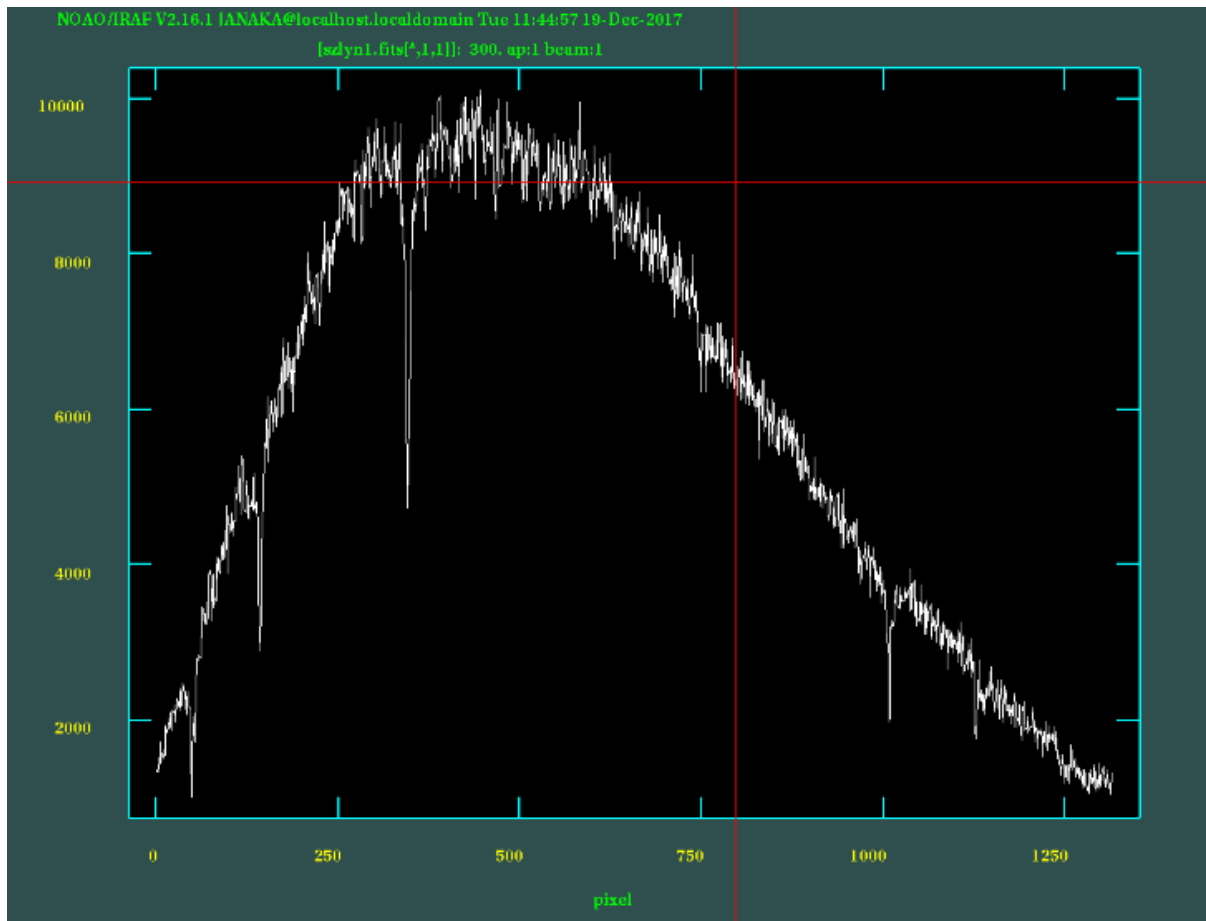
Figure 5.4 Extracted 1D spectrum in Pixels

5.1.2 Wavelength Calibration

For each spectral image of the star, a comparison spectra is formed in the CCD by an Ar-Ne lamp.
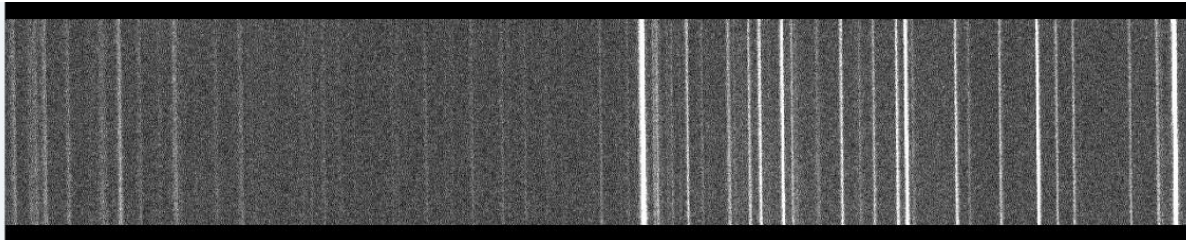
Figure 5.5 Ar-Ne comaprison spectra generated by Spectrograph

Therefore the 1D image of the comparison spectra was extracted using the previously discussed 1D extraction method.
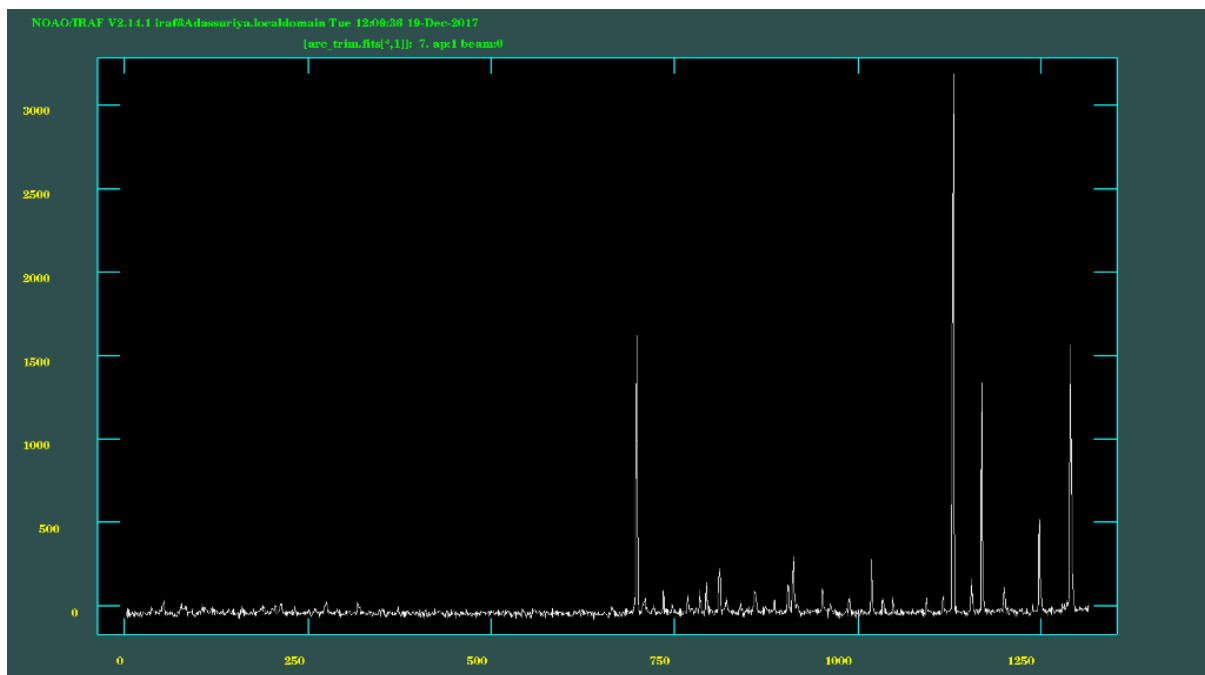
Figure 5.6 1D spectra of Ar-Ne comparison lamp

Then two wavelengths in 1D comparison spectra were identified with the help of Ar-Ne lamp emission spectra which is provided by the manufacturer (Appendix, figure 9.1) in the spectrograph guide book. The wavelengths are identified by comparing the peak separation and the intensities of the extracted spectrum and the spectral energy distribution in the guide book. The wavelength values of identified 2 peaks of the comparison spectrum were assigned to the

corresponding peaks using the package "identify" in IRAF. Then the corresponding task was executed to convert the pixel values to wavelength in the comparison spectra.
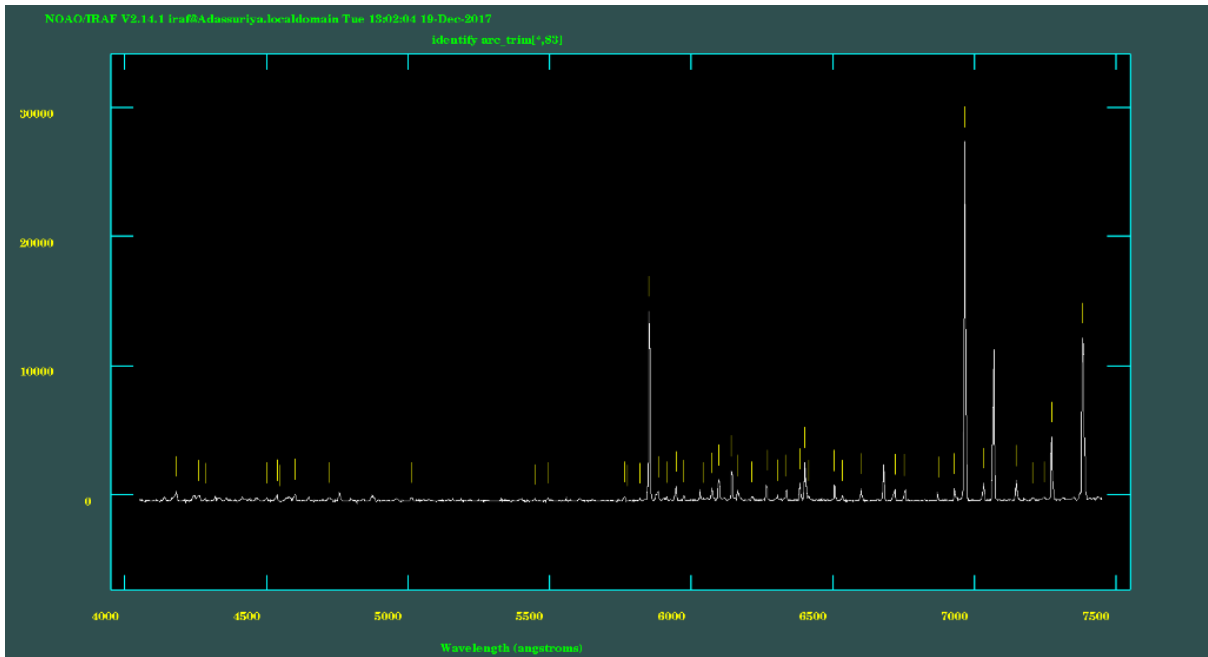
Figure 5.7 Wavelength identification of comparison lamp

Then extrapolated dispersion solution for whole region was generated to compare the accuracy of the pixel to wavelength conversion.
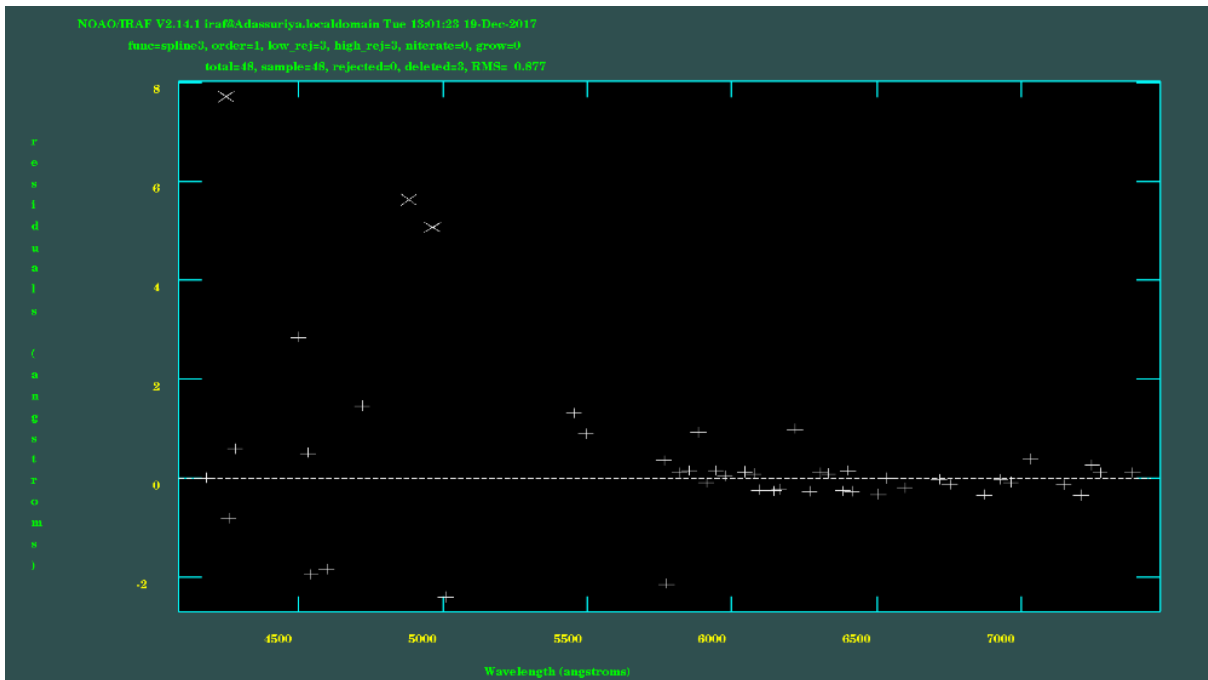
Figure 5.8 Extrapolated dispersion solution

Then the pixel values of the extracted 1D spectrum of the star was assigned wavelength values by referring two calibrated spectrums of the lamp using the package "refspectra". Finally this wavelength solution was applied to the stellar 1D spectrum by running "dispcor" command.
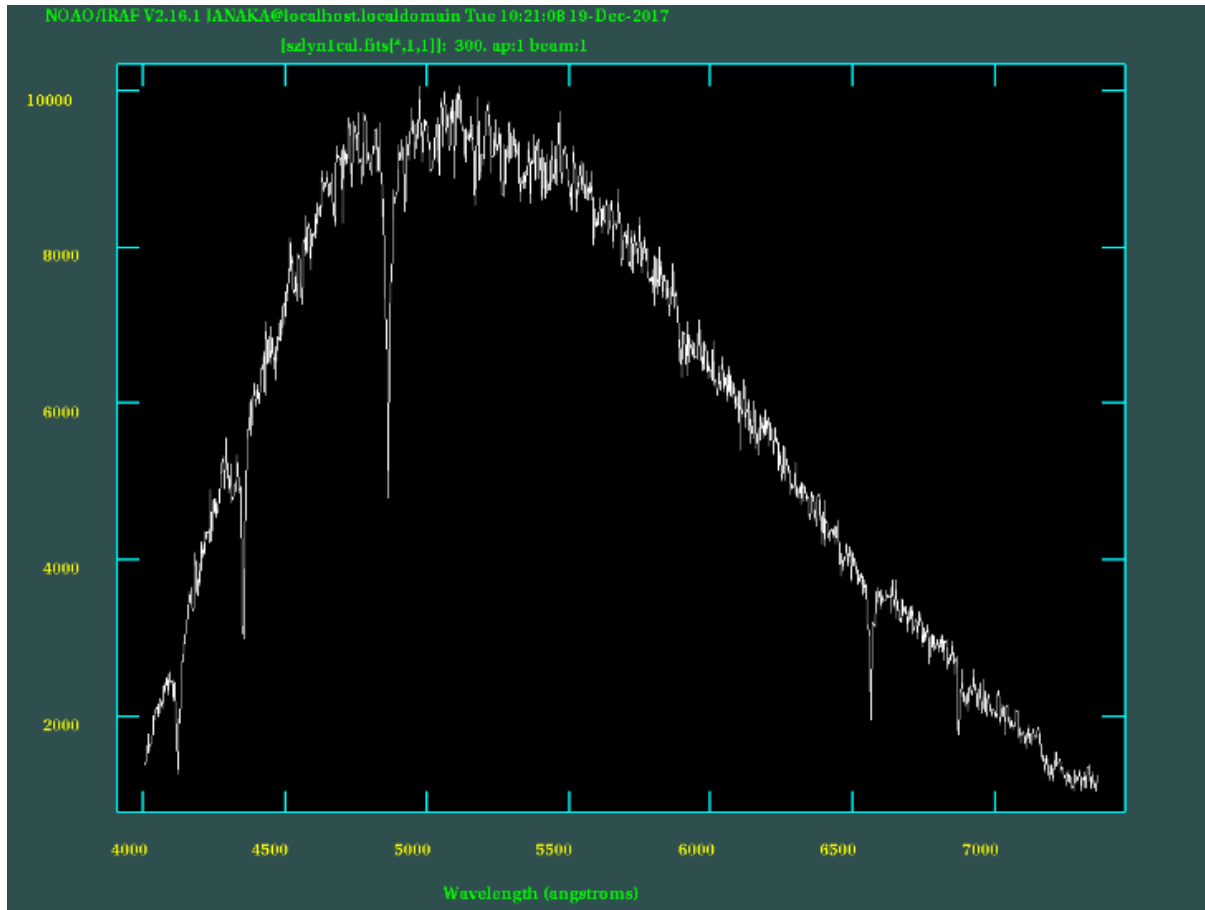
Figure 5.9 Generated 1D spectrum in wavelength frame

5.1.3 Normalization to Stellar Continuum

To the convenience of analysis, the absorption lines were conclude to a mathematical model. So the equivalent width, full width at half maximum and many more properties of the peaks were measured. In order to measure those parameters of the peaks the 1D spectrum was converted to a continuum. In order to do so a reference level was created by running the "continuum" command in IRAF "kpnoslit: package.

When running the task continuum, bends of the spectrum, the number of the data points in the sample and also the number of low rejected points were considered more carefully. In this situation a more complex functions were tried to apply such as 'spline3'. Usually the RMS values were at higher levels. But RMS values can be reduced by applying higher orders for the function. When applying higher orders, there are limitations according to the behavior of

24

the data points. The reduction of data points should be minimized. For the minimum case at least number of 10 data points are required for the analysis.
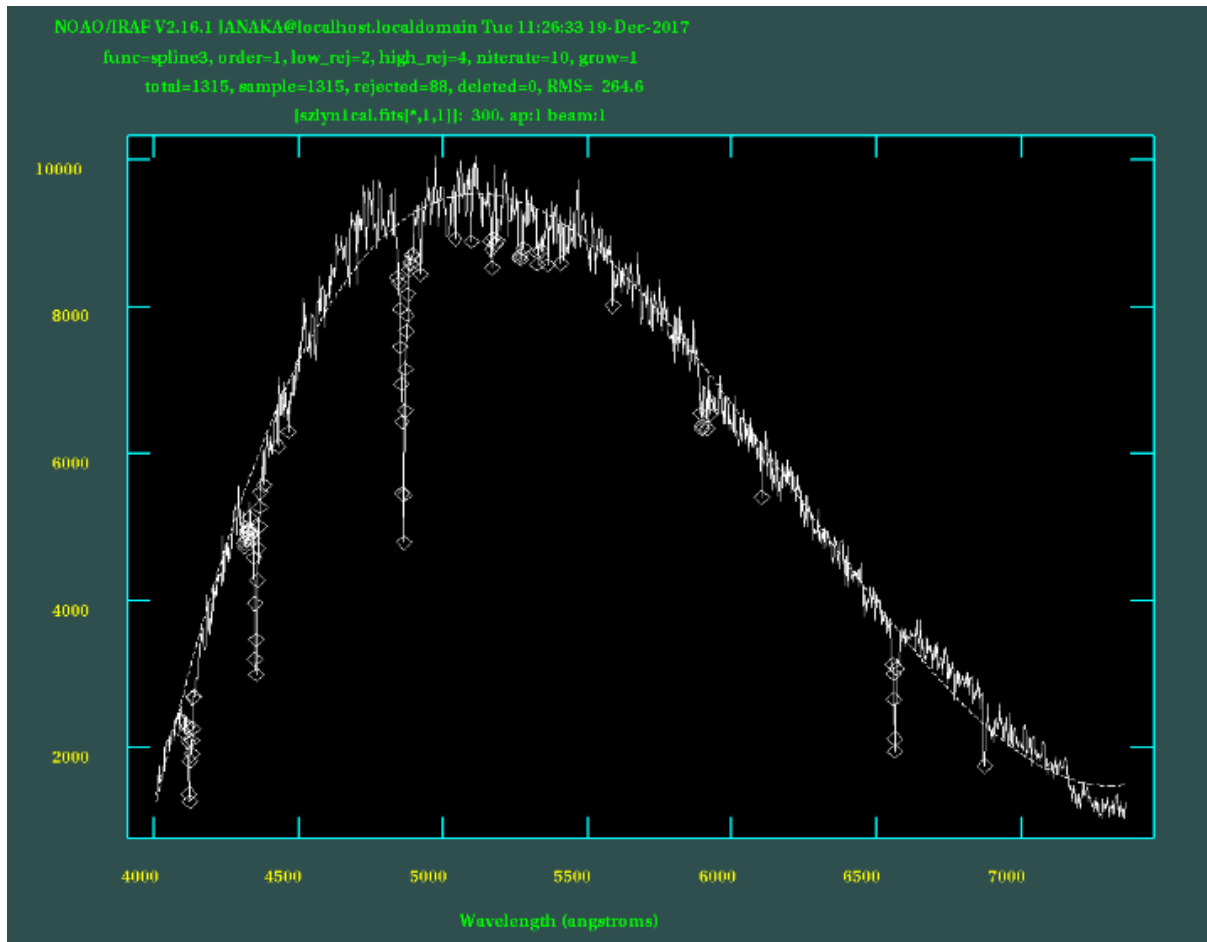
Figure 5.10 Selected data points to generate continuum
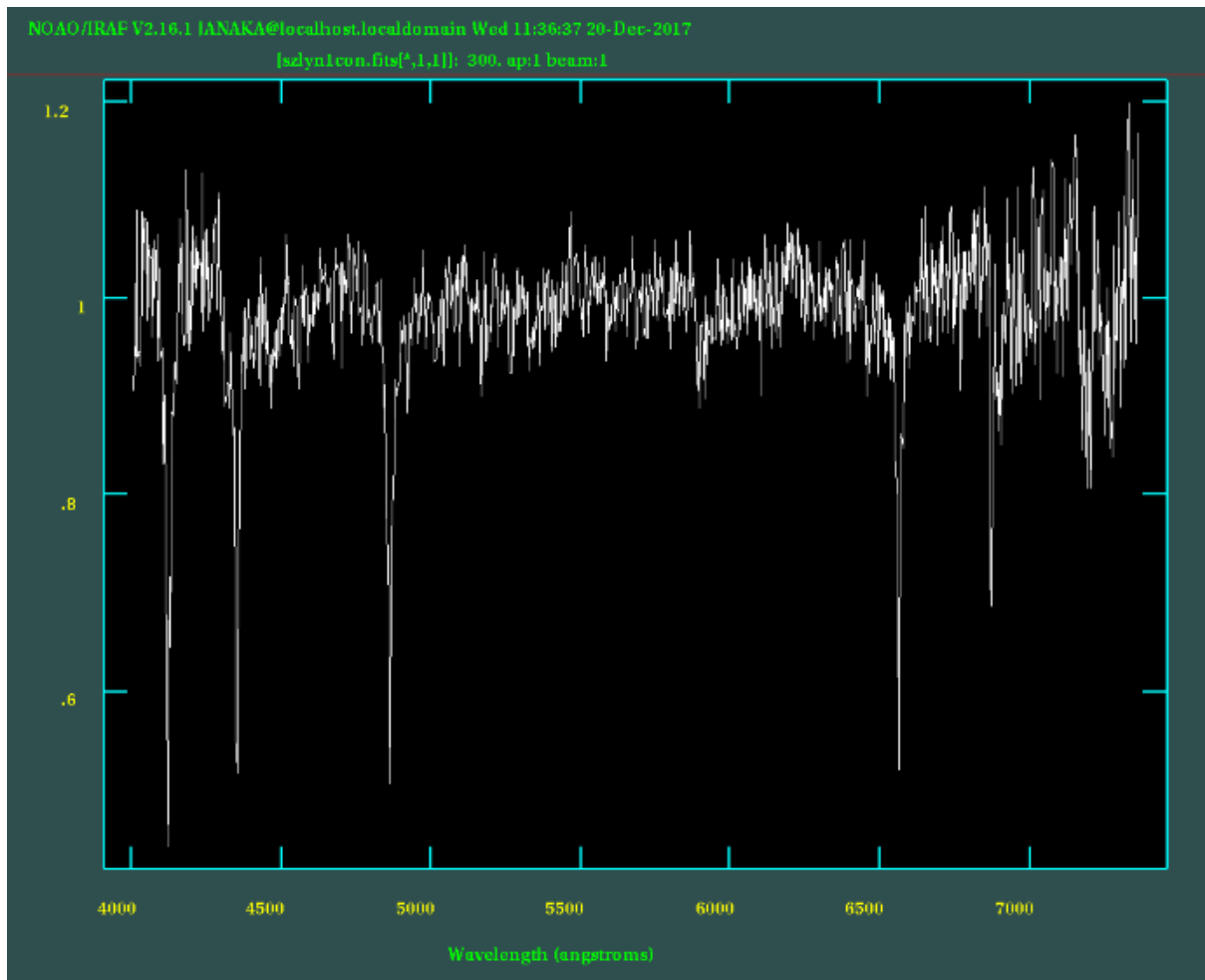
Figure 5.11 Normalized Stellar continuum

5.1.4 Gaussian Fit method

In order to find the equivalent width and the full width at half maximum of the peaks the option of fitting a Gaussian profile on "splot" menu was used. Symmetric Gaussian profiles were fitted to each and every absorption line. Then the equivalent width and the full width at half maximum was recorded.
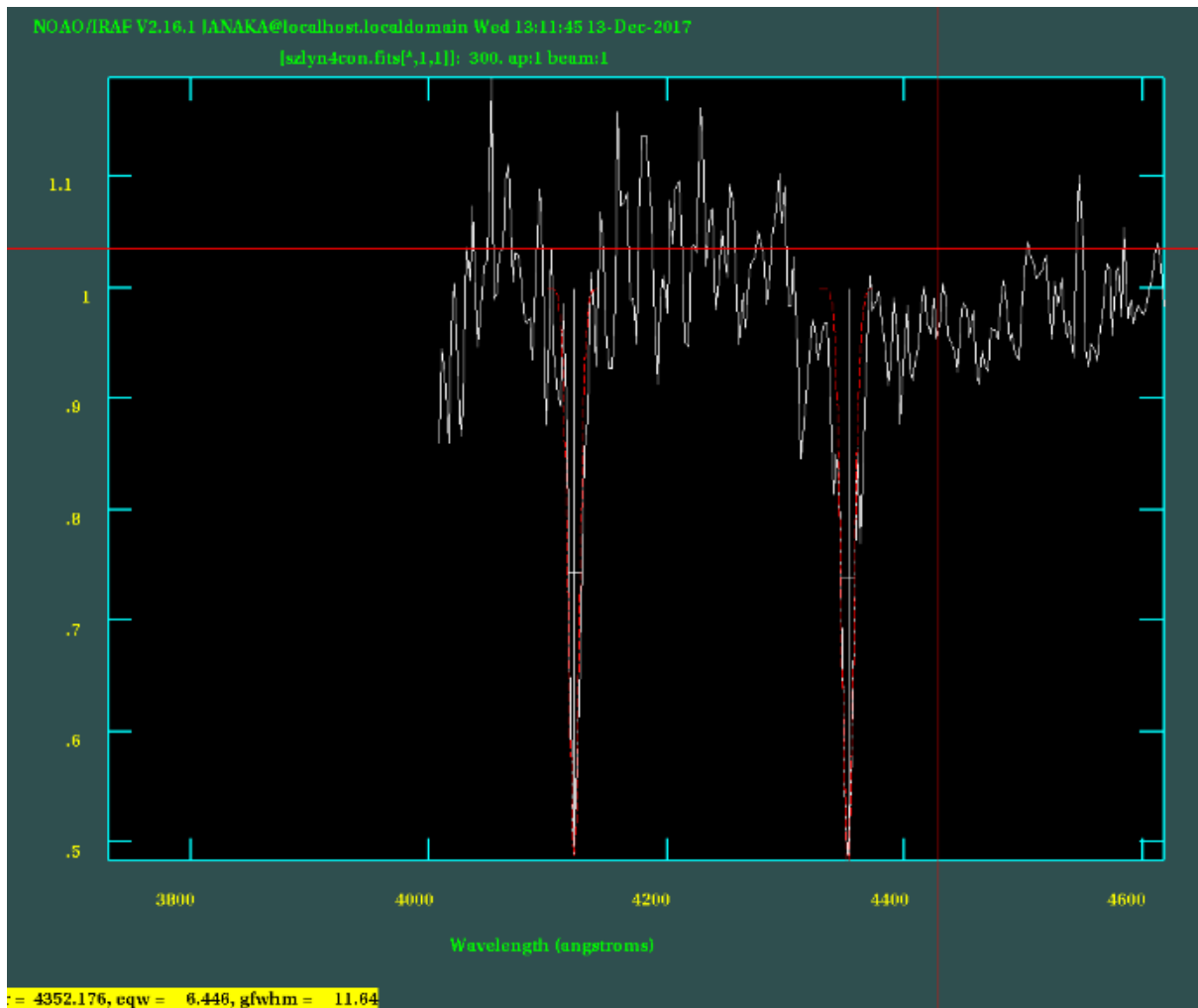
Figure 5.12 Interpolated Gaussian profiles

5.2 Phase Calculation

First the observation time and date were obtained from the image using the command "imhead l+". As the date and time was in local time frame they were converted in to UTC frame. Then they were converted in to Heliocentric Julian Dates (HJD). Then the phases of the images were calculated considering the period of the star as 0.1205 days (Moffett J. et.al, 1987).

5.3 Identifying peaks of the spectra

The chemical elements which formed the absorption lines that were appeared in the calibrated spectrum of the star (HD67930) are unknown. But every minima that formed in the synthetic spectrum was due to specific chemical element. So they were identified using the wavelength of minima's obtained from the continuum and the emission line wavelengths of elements that are possible to exist in an "A type star".

6   RESULTS AND ANALYSIS

For the obtained wavelengths of minima's absorption lines, identified absorption lines. (David R. et.al, 1995)

Table 6.1 Wavelength Identification of Absorption lines

Wavelength reading of minima's obtained from continuum (^{0}A) ($\pm 1.275\ ^0$A)	Identified absorption line	Wavelength of the identified absorption line (^{0}A)	Wavelength value with errors
4122.648	Unknown		$(4122 \pm 1)\ ^0$A
4351.110	H Gamma	4332.21	$(4351 \pm 1)\ ^0$A
4862.036	H Beta	4861.05	$(4862 \pm 1)\ ^0$A
6560.036	H Alpha	6563.78	$(6560 \pm 1)\ ^0$A
6869.644	$Fe^{3}+$	4122.02	$(6869 \pm 1)\ ^0$A

28

Table 6.2 Determined Eqw and FWHM values

Image Frame	4122.648 ^{0}A (±1.275 ^{0}A)		4351.11 ^{0}A H(γ) (±1.275 ^{0}A)		48H62.036 ^{0}A H(β) (±1.275 ^{0}A)		6560.318 ^{0}A H(α) (±1.275 ^{0}A)		6869.644 ^{0}A (Fe^{3+}) (±1.275 ^{0}A)	
1	5.987	9.888	6.549	12.720	8.457	16.110	4.355	8.352	3.391	10.190
2	5.409	9.305	7.229	13.940	7.708	15.560	4.518	9.264	2.529	7.279
3	5.222	9.053	5.964	11.520	7.729	14.940	5.892	11.880	2.850	7.116
4	5.944	10.920	6.446	11.640	7.059	14.340	4.772	9.211	3.108	10.370
5	5.353	9.402	7.251	14.470	8.381	17.720	5.124	9.419	3.558	9.772
6	7.038	13.750	5.510	10.940	7.155	14.720	4.122	10.710	3.097	8.993
7	6.070	11.170	5.881	11.750	6.899	14.190	5.236	10.780	2.909	7.832
8	5.893	11.990	6.168	13.070	7.608	17.730	4.297	8.537	2.674	7.080
9	5.530	10.600	6.179	12.470	8.246	12.130	4.999	11.250	3.508	8.204
10	4.610	8.382	5.472	12.030	8.716	18.350	3.893	6.901	2.871	9.056
11	5.230	9.620	6.322	12.010	7.421	15.170	4.870	10.350	3.388	10.120
12	6.426	12.820	5.387	10.990	7.351	15.800	4.399	9.581	3.652	10.060
13	5.846	10.060	5.935	11.600	7.181	14.760	4.455	10.320	4.186	10.810
14	7.711	15.160	6.552	12.970	7.237	15.010	5.710	11.880	2.591	7.716
15	6.543	11.300	6.360	12.100	9.317	17.830	5.457	10.450	3.285	6.356
16	7.743	12.020	7.013	13.000	8.908	17.920	5.568	12.600	4.395	9.221
17	8.753	12.530	7.844	13.440	9.875	18.880	8.246	14.570	8.257	10.460

Table 6.3 Local time to HJD time conversion

Local date	Local Time	UTC Date	UTC	HJD	phase
2016.10.17	23:08:32	2016.10.17	17:38:32	2457679.235	0.31613697
2016.10.17	23:13:34	2016.10.17	17:43:34	2457679.239	0.34517751
2016.10.17	23:18:36	2016.10.17	17:48:36	2457679.242	0.37413509
2016.10.17	23:23:38	2016.10.17	17:53:38	2457679.246	0.40317563
2016.10.17	23:28:40	2016.10.17	17:58:40	2457679.249	0.4321332
2016.10.17	23:33:41	2016.10.17	18:03:41	2457679.253	0.46109077
2016.10.17	23:38:43	2016.10.17	18:08:43	2457679.256	0.49004835
2016.10.17	23:43:45	2016.10.17	18:13:45	2457679.26	0.51917186
2016.10.17	23:48:47	2016.10.17	18:18:47	2457679.263	0.54812944
2016.10.17	23:53:49	2016.10.17	18:23:49	2457679.267	0.57708701
2016.10.17	23:58:50	2016.10.17	18:28:50	2457679.27	0.60596161
2016.10.18	00:03:52	2016.10.17	18:33:52	2457679.274	0.63500215
2016.10.17	00:08:54	2016.10.17	18:38:54	2457679.277	0.66395972
2016.10.17	00:13:56	2016.10.17	18:43:56	2457679.281	0.69300027
2016.10.17	00:18:58	2016.10.17	18:58:58	2457679.284	0.72204081
2016.10.17	00:23:59	2016.10.17	18:53:59	2457679.287	0.75091541
2016.10.17	00:29:01	2016.10.17	18:59:01	2457679.291	0.77995596

6.1 Plots for absorption lines

6.1.1 Absorption line on 4122.648 ^{0}A
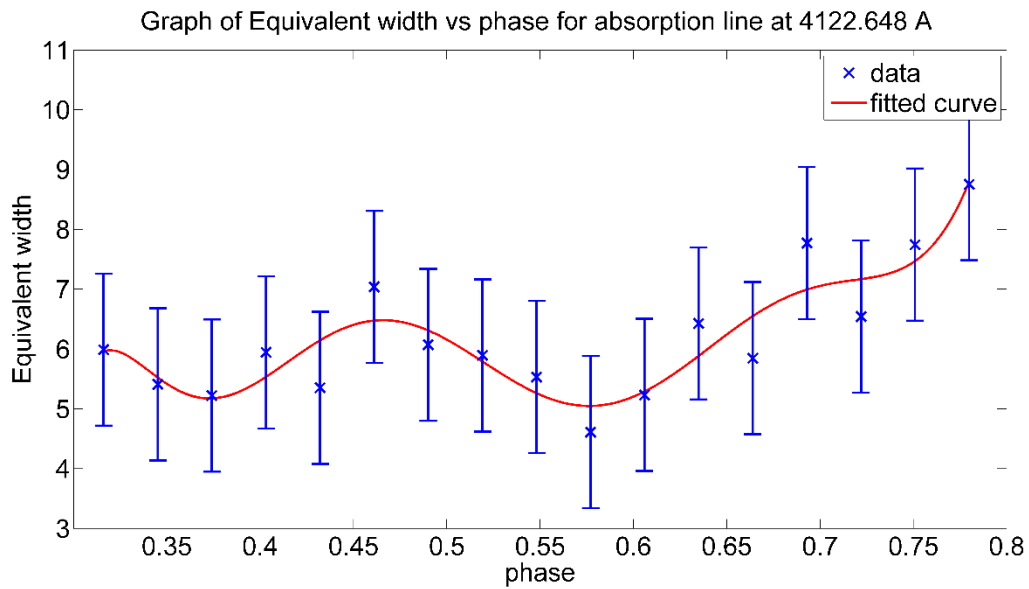
Figure 6.1 Graph of Equivalent width vs. phase for absorption line at 4.122.648 ^{0}A
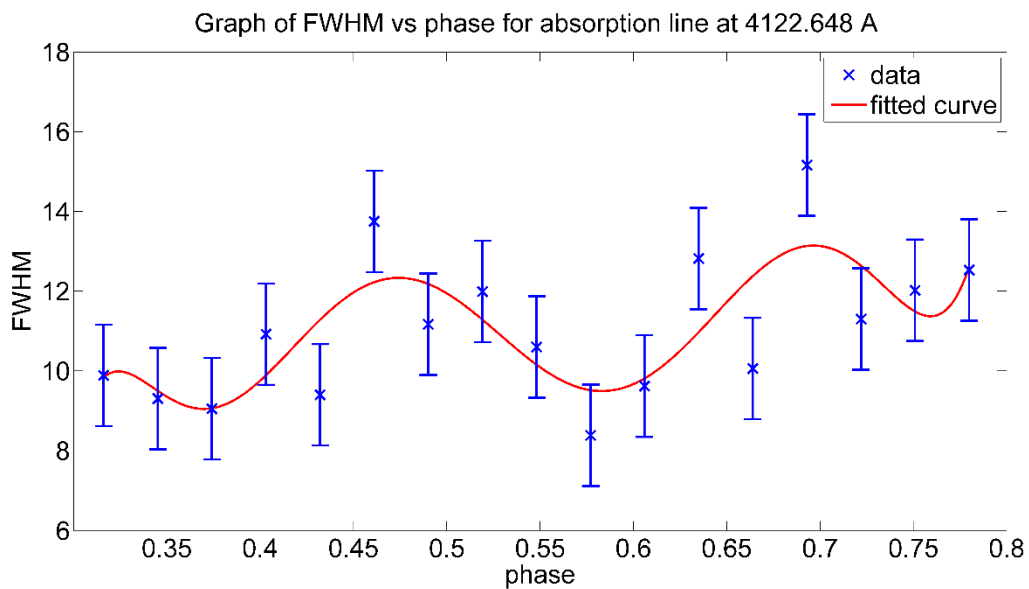
Figure 6.2 Graph of FWHM vs. phase for absorption line at 4.122.648 ^{0}A

6.1.2 H Gamma absorption line
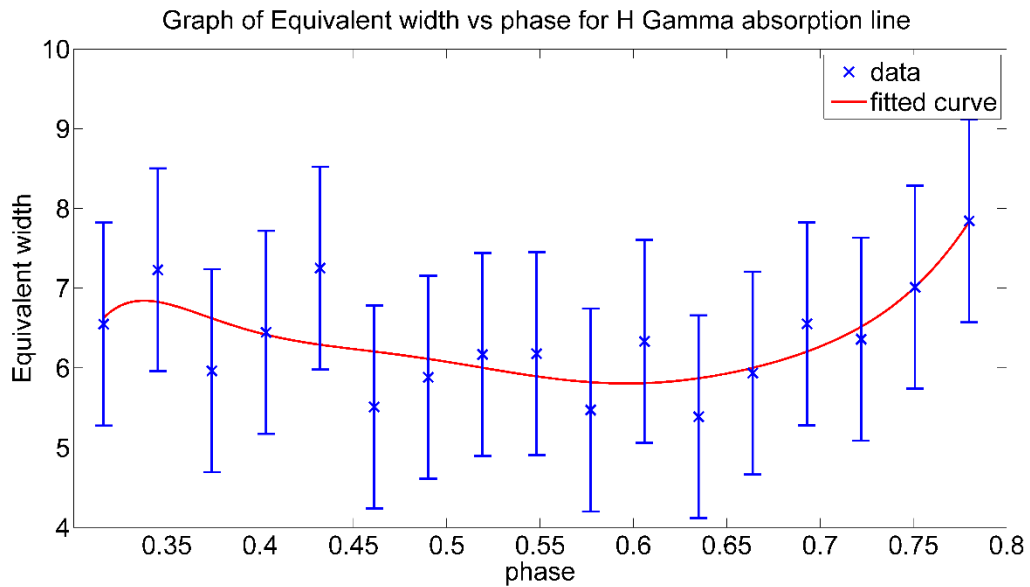
Figure 6.3 Graph of Equivalent width vs. phase for H Gamma absorption line
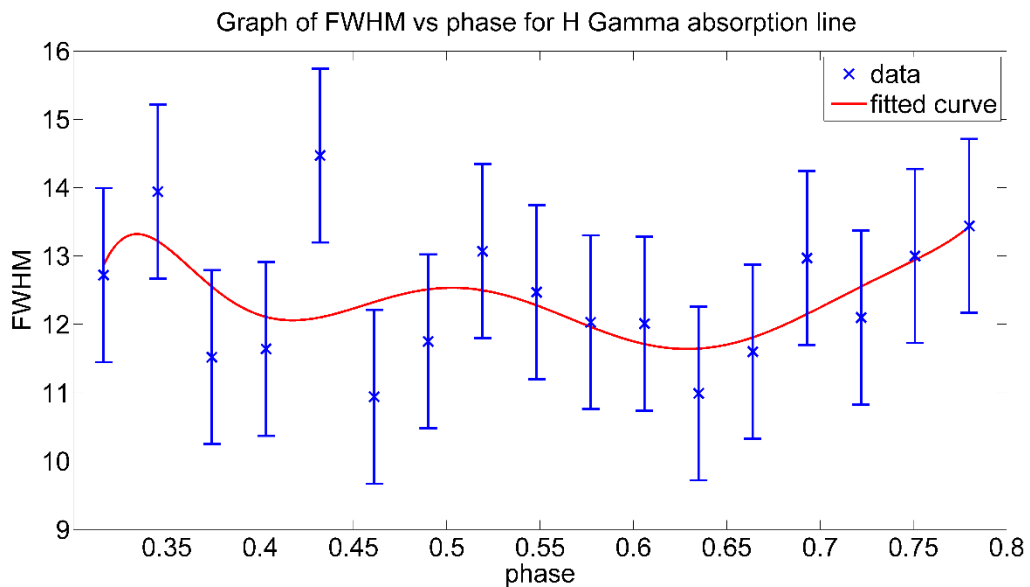
Figure 6.4 Graph of FWHM vs. phase for H Gamma absorption line

6.1.3 H Beta Absorption line
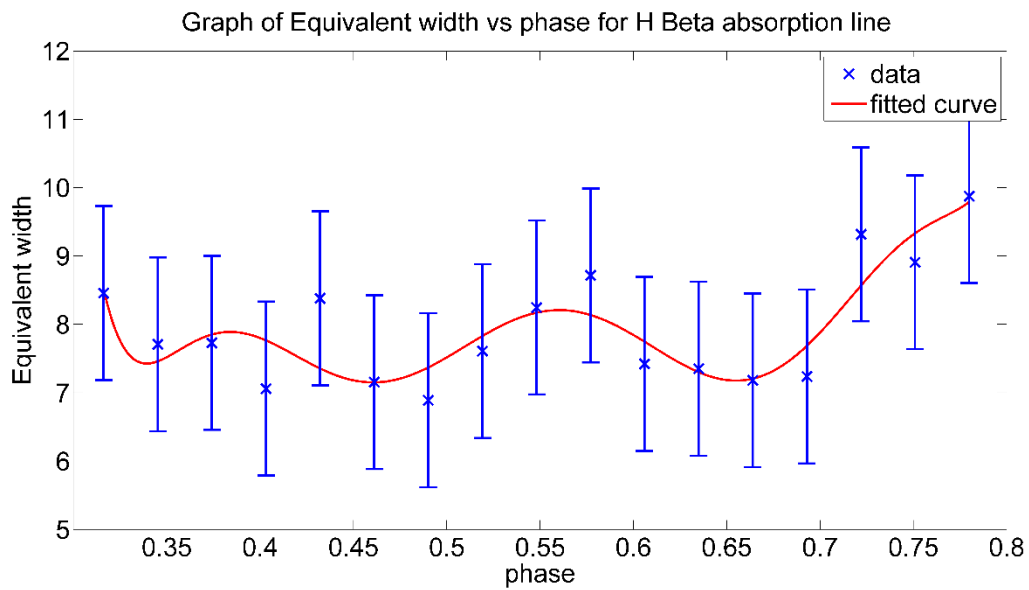
Figure 6.5 Graph of Equivalent width vs. phase for H Beta absorption line
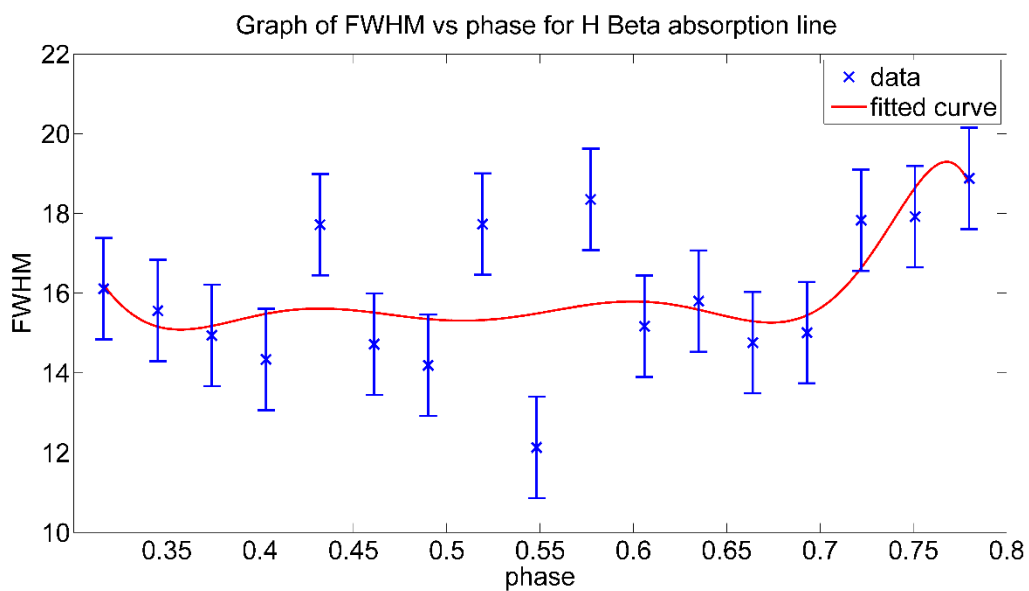
Figure 6.6 Graph of FWHM vs. phase for H Beta absorption line

6.1.4   H Alpha absorption line
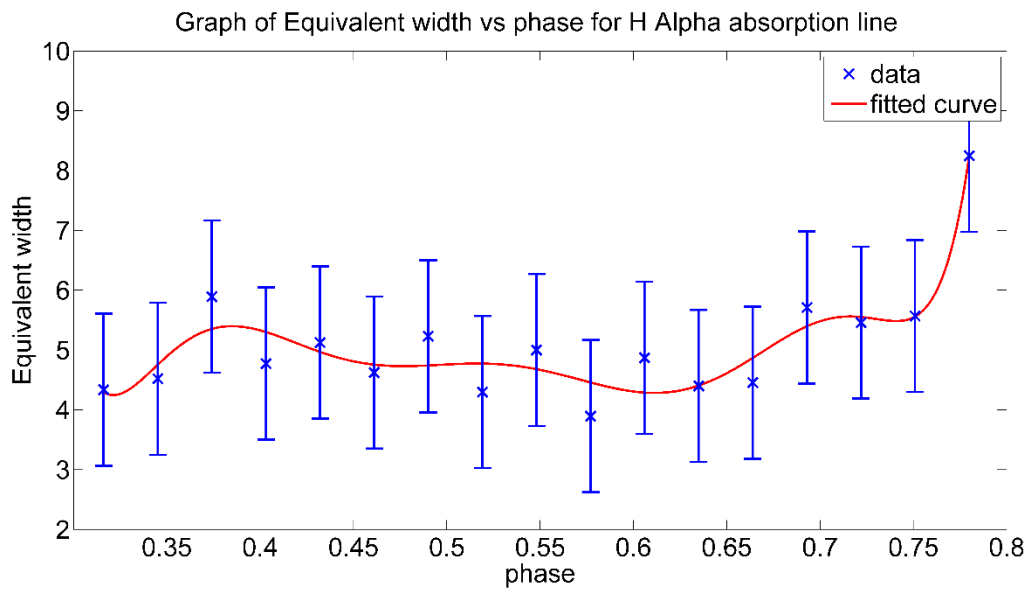
Figure 6.7 Graph of Equivalent width vs. phase for H Alpha absorption line
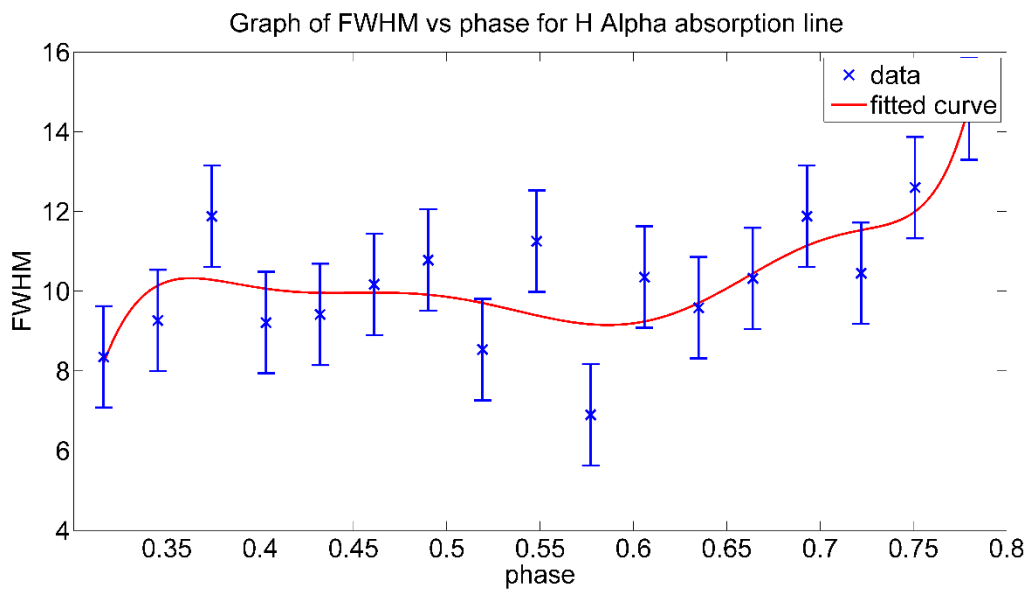
Figure 6.8 Graph of FWHM vs. phase for H Alpha absorption line

6.1.5   Fe³⁺ Absorption line
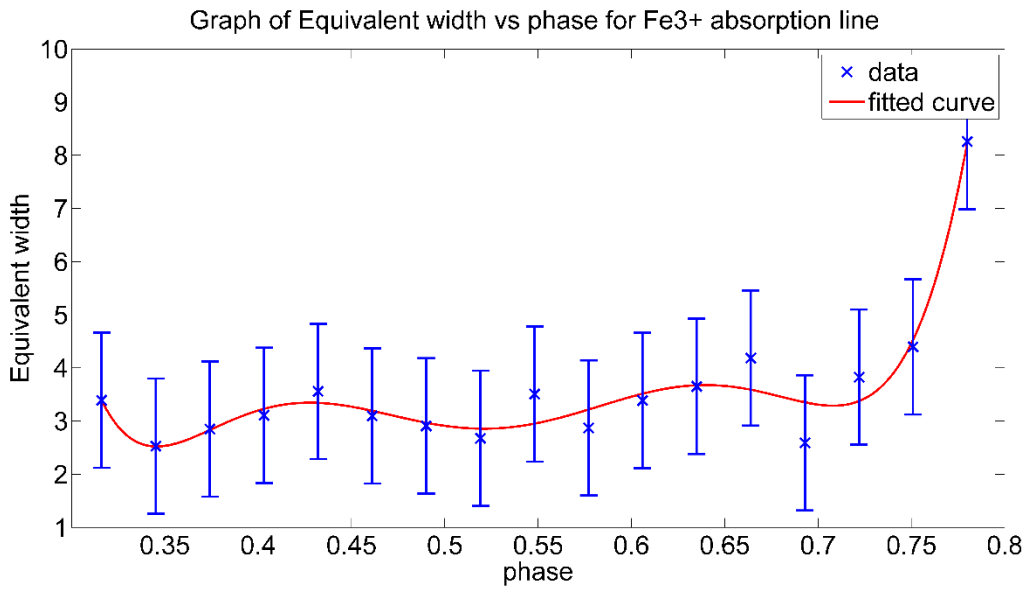
Figure 6.9 Graph of Equivalent width vs. phase for Fe3+ absorption line
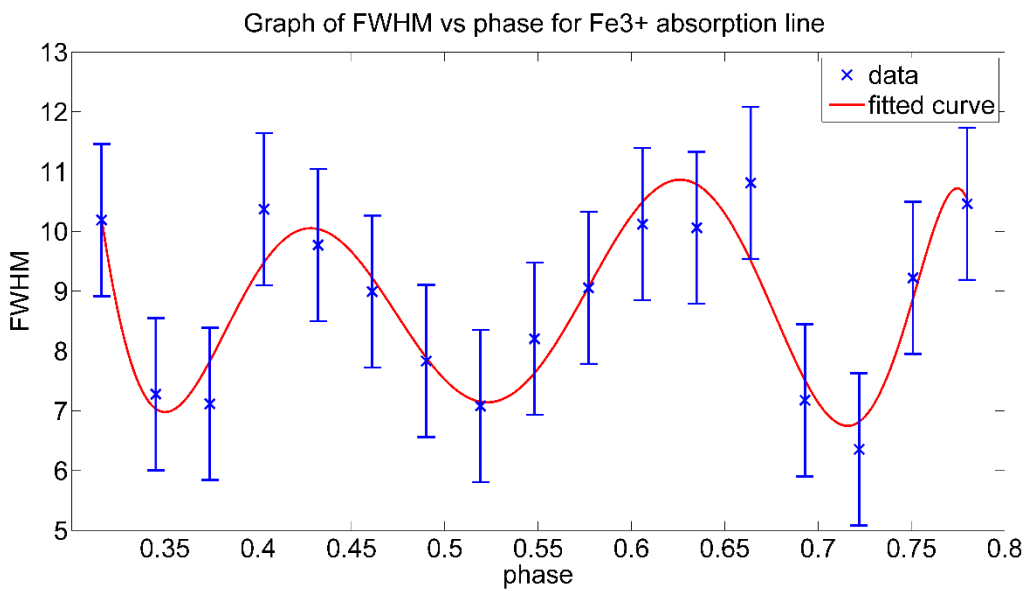
Figure 6.10 Graph of FWHM vs. phase for Fe3+ absorption line

6.2 Photometric Pulsation curve of the star
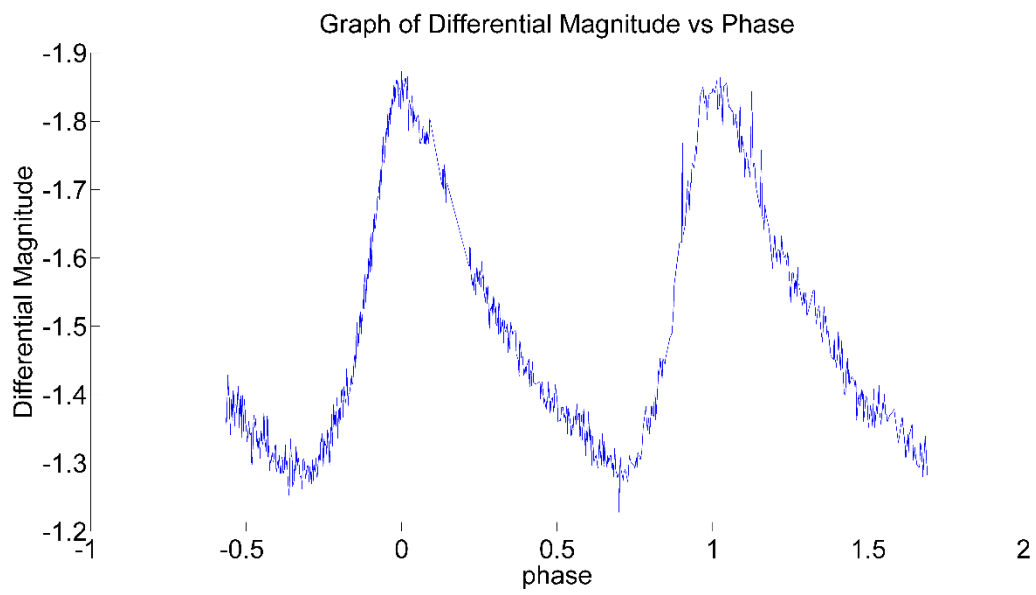
Figure 6.11 Photometric periodic curve of the HD67930 star

7 DISCUSSION

The spectroscopic study was conducted on HD67930 high amplitude δ Scuti type star which is located on SZ Lyncis constellation and has a pulsation period of 0.1205 days (Soliman et al., 1986).

Basic image reduction such as subtraction of bias frame and flat field correction was done using Image Reduction and Analysis Facility (IRAF).

The response function of the spectrograph was determined from the flat field spectrum (figure 5.2) and it was observed that the accuracy of the spectrograph is much higher on the middle of the spectrograph and its decreasing to the both left and right ends of the spectrograph.

It was determined that the elements Hydrogen (H) and Iron (Fe) exist on the HD67930 as absorption lines corresponding to those elements were observed. It was a quite significant phenomenon to observe absorption lines of hydrogen, as an absorption spectrum of the sun doesn't contains hydrogen lines. It is obvious that the energy on the surface is much higher on HD67930, as   it is an "A" type star which has a surface temperature of 9000K while our sun is a "G" type star which has a surface temperature of 5000k. As Ionization energy of hydrogen is higher than other elements, the sun doesn't contains sufficient energy to emit hydrogen spectrum while HD67930 has sufficient energy to ionize hydrogen atom. The absorption line corresponding to Fe^{3+} was contained in the observed absorption spectra. Iron exist as Fe^{3+} in the star atmosphere. Which is Iron has almost ionized to its 3rd state, as HD67930 has a considerably high surface energy.

Wavelengths of absorption lines corresponding to H Alpha, H Beta and Fe^{3+} was determined accurately. It was difficult to identify the 1st absorption line and to determine the H Gamma line as it has deviated significantly from the theoretical value. This was happened due to lack of spectral lines on the left side of the observed emission spectra of the Ar-Ne comparison lamp (figure 5.6). As there are less number of spectral lines in the left side of the observed comparison spectrum to identify from comparison spectrum provided by manufacturer (Appendix, figure 9.1) the accuracy of the determined wavelengths are less on the left end. So it was difficult to determine the 1st absorption line and the determined H Gamma line has deviated from real value.

The conversion of the local time frame to heliocentric Julian Dates (HJD) was done to calculate the phase of the images. As most of the time parameters of the stars are defined on HDJ time frame.

The obtained absorption minima's were modeled in to a Gaussian profile in order to have a mathematical idea. Then the equivalent width and the full width at half maximum for each and every absorption lines were tabulated and potted against phase.

The images of one periodic cycle of the HD67930 was analyzed throughout this project. As photometric curve (figure 6.11) indicates that the pulsation has minimum Differential Magnitude around 0.6 and 0.7 while the plotted equivalent width vs. phase and FWHM vs. phase curves have minimum EQW and FWHF values around the same phase.

The most of the plotted equivalent width vs. phase and FWHM vs. phase curves shows rising trend after the minima while the photometric curve shows the same trend. Which illustrate that the photometry and the spectroscopic data have same qualities even though the observation analysis processes were completely different.

8 CONCLUSION

The main purpose of this research was to determine the interior of a star. So it was determined that HD67930 emits 5 emission spectra belong to H Alpha, H Beta, H Gamma and Fe^{3+} . The determined corresponding wavelengths of absorption lines were H(α) = (6560 ± 1) ^{0}A, H(β)= (4862 ± 1) ^{0}A, H(γ) = (4351 ± 1) ^{0}A and Fe^{3+} = (6869 ± 1) ^{0}A. Further investigation is required on more periods of the star to have a good understanding on its spectroscopic data.

And the same procedure can be applied to other δ Scuti type stars to analyze the interior of the star through spectroscopy. Furthermore investigation can be conduct with much advanced telescopes, spectrographs and etc. to improve the accuracy of the result.

9 REFERENCES

Gazeas K. D., Niarchos P. G., The Light-Time Effect in SZ Lyn, ASP Conference Series, Vol. 335, (2005), 297 – 301

Seaman R., Anderson E., An Introduction User's Guide to IRAF Scripts, National Optical Astronomical Observatories, (1989)

Gazeas K. D., Niarchos P. G., Boutsia K. A. , SZ Lyn: New BVRI CCD Observations and Improved Pulsation and Orbital Elements., Asustrian Academy of Science, Vol. 144 (2004), 26 – 34

Paparo M., Szeidl B., Hamid A. M., The High Amplitude Delta Scuti Star SZ Lyncis Revisited, Astrophysics and Space Science 149 (1988), 73 – 82

Kurtz D. W., 2005, "Asteroseismology: Past, Present and Future", Journal of Astrophysics and Astronomy, **26** , 123 – 138

Moffett J. et.al Orbital and Photometric properties of HD67930 (1987), The Astronomical Journel

UTC to HJD converter. [Online]Available at: http://britastro.org/computing/applets_dt.html [Accessed 29 October 2017]

David R. Lide, Handbook of Physics and Chemistry,76th edition. 1995,vol 10

APPENDIX

Matlab code used for plot the photometric curve of Differential Magnitude vs phase

```
x=Phase1
y=DifMag;
%plot(x,y)

hold on
[lim1 indx]=min(y(1:400));
% plot(x(indx),lim1,'ro')
set(gca,'fontsize',22)
plot(x-x(indx),y)

set(gca, 'YDir', 'reverse')
title('Graph of Differential Magnitude vs Phase')
xlabel('phase')
ylabel('Differential Magnitude')
```

Matlab code used for plot the curve of Equivalent width, FWHF vs. phase

```
clc; clear all;
close all;
eq1=[5.987 5.409 5.222 5.944 5.353 7.038 6.07 5.894 5.53 4.61 5.23 6.426
5.846 7.771 6.543 7.743 8.753];
gf1=[9.888 9.305 9.053 10.92 9.402 13.75 11.17 11.99 10.6 8.382 9.62 12.82
10.06 15.16 11.3 12.02 12.53];
eq2=[6.549 7.229 5.964 6.446 7.251 5.51 5.881 6.168 6.179 5.472 6.332 5.387
5.935 6.552 6.36 7.013 7.844];
gf2=[12.72 13.94 11.52 11.64 14.47 10.94 11.75 13.07 12.47 12.03 12.01
10.99 11.6 12.97 12.1 13 13.44];
eq3=[8.457 7.708 7.729 7.059 8.381 7.155 6.889 7.608 8.246 8.716 7.421
7.351 7.181 7.237 9.317 8.908 9.875];
gf3=[16.11 15.56 14.94 14.34 17.72 14.72 14.19 17.73 12.13 18.35 15.17 15.8
14.76 15.01 17.83 17.92 18.88];
eq4=[4.335 4.518 5.892 4.772 5.124 4.622 5.231 4.297 4.999 3.893 4.87 4.399
4.455 5.71 5.457 5.568 8.246];
gf4=[8.352 9.264 11.88 9.211 9.419 10.17 10.78 8.537 11.25 6.901 10.35
9.581 10.32 11.88 10.45 12.6 14.57];
eq5=[3.391 2.529 2.85 3.108 3.558 3.097 2.909 2.674 3.508 2.871 3.388 3.652
4.186 2.591 3.825 4.395 8.257];
gf5=[10.19 7.279 7.116 10.37 9.772 8.993 7.832 7.08 8.204 9.056 10.12 10.06
10.81 7.176 6.356 9.221 10.46];
cjd=[0.316136968 0.345177514 0.374135086 0.403175628 0.432133201
0.461090773 0.490048345 0.519171865 0.548129437 0.57708701 0.605961608
0.635002154 0.663959723 0.693000269 0.722040814 0.750915413 0.779955959];
e=[1.272 1.272 1.272 1.272 1.272 1.272 1.272 1.272 1.272 1.272 1.272 1.272
1.272 1.272 1.272 1.272 1.272];


% plot(cjd,eq4,'r-');
% hold on;
% plot(cjd,gf4,'-');
% hold off;
```

```
[xData, yData] = prepareCurveData( cjd, eq1 );

% Set up fittype and options.
ft = fittype( 'poly8' );

% Fit model to data.
[fitresult, gof] = fit( xData, yData, ft );
set(gca,'fontsize',22)
h1 = plot( fitresult, xData, yData,'bx');
set(h1,'linewidth',2,'MarkerSize',12);
% Plot fit with data.
% legend(  ' ', 'untitled fit 1', 'Location', 'NorthEast' );
 hold on
h=errorbar(cjd,eq1,e,'bx');
set(h,'linewidth',2,'MarkerSize',12)
title('Graph of Equivalent width vs phase for absorption line at 4122.648 A
')
xlabel('phase')
ylabel('Equivalent width')
[a,b]=min(fitresult(xData))
xData(b)
```

Calibration spectrum provided by manufacturer of Spectrograph

Ar - 7635.11 Å

Ar - 7503.87 Å

Ar - 7272.94 Å

Ar - 7067.22 Å

Ar - 6965.43 Å

Ar - 6677.28 Å

Ne - 6402.25 Å

Ne - 6143.06 Å

Ne - 5852.49 Å

calibration

Ar - 4764.87 Å

Ar - 4510.73 Å

Ar - 4200.67 Å

Ar - 3948.98 Å
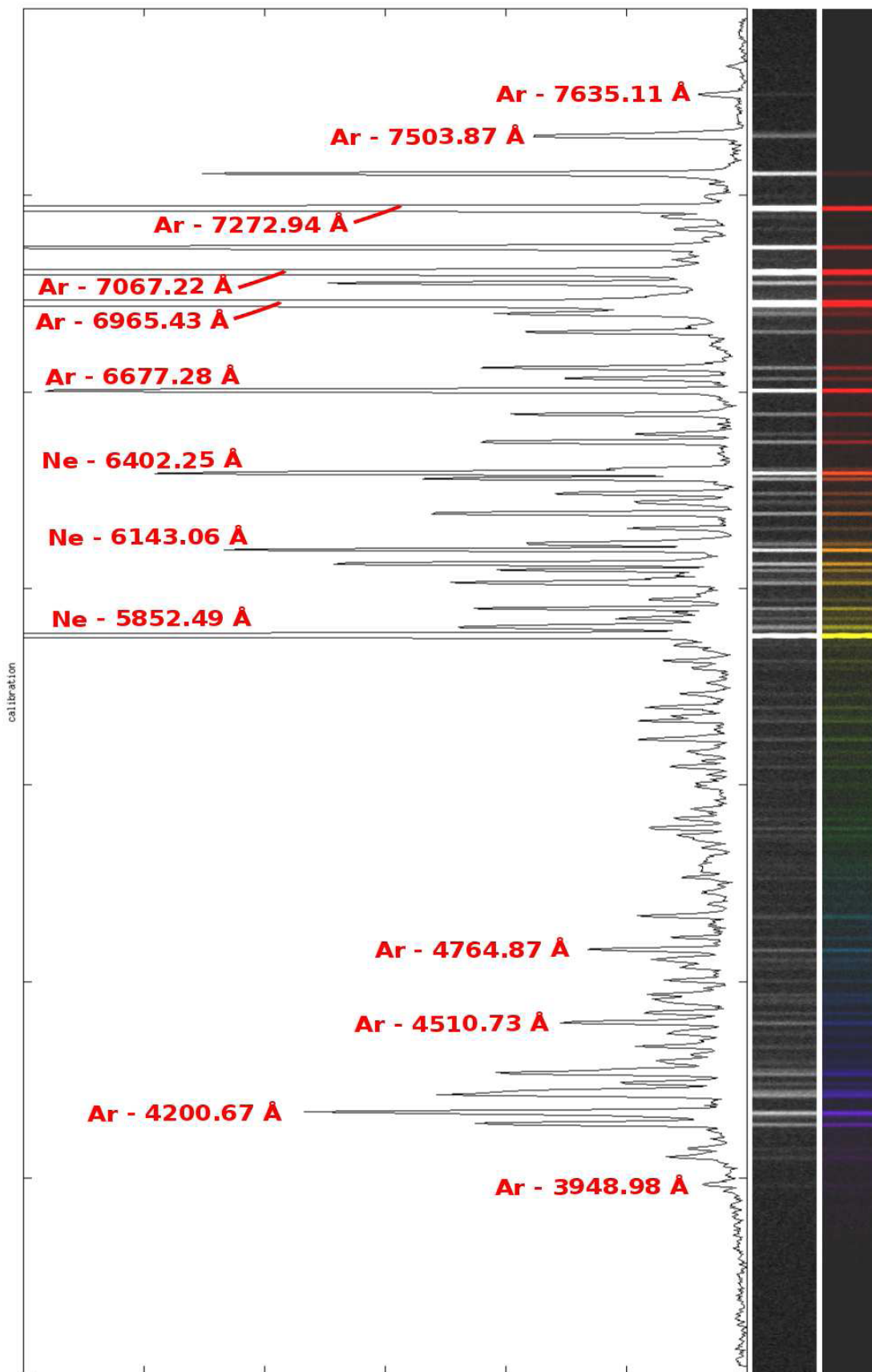
Figure 9.1 Calibration spectrum provided by the manufacturer of spectrograph